CHAPTER 6

RESULTS AND DISCUSSIONS

6.1 Disruption of *Chlorella ellipsoidea* TISTR 8260

6.1.1 Effect of Superficial Gas Velocity

First, this experiment results depict the effect of superficial gas velocity in the absence of superficial liquid velocity and agitation speed on the cell disruption. Superficial gas velocities were varied between 10 and 40 cm/min. When superficial gas velocities were increased from 10 cm/min to 20 cm/min, the percentage of cell ruptured was decreased from 41.8% to 18.3% (Figure 6-1). However, when the superficial gas velocity was increased to 40 cm/min, percentage of cell ruptured rose slightly. Such result could be confirmed by the rate of cell disruption (Figure 6-2), change of cell volume at various operating time (Figure 6-3), amount of Chlorophyll A released (Figure 6-4) and morphological change of cells (Figure 6-5).

Regarding to the obtained results two mechanisms of cell disruption could be implied. The mechanisms were (1) the motion of glass bead providing particle-particle interaction and particle-cell interaction and (2) shear stress generated from the motion of air bubbles.

The motion of glass beads, which were employed as grinding media, is could be implied to take place because superficial gas velocity employed in this work was high enough to induce their fluidizing state. The following equation is used to verify this assumption;

$$\frac{U_{mf}}{U_{mfo}} = 1 - 376 U_g^{0.327} \mu_\ell^{0.227} d_p^{0.213} (\rho_s - \rho_\ell)^{-0.423} \qquad (6.1\text{-}1)$$

The U_{mfo} can be calculated from Wen and Yu's correlation (1996) for liquid-solid fluidized beds.

$$\mathrm{Re}_{mfo} = \sqrt{(33.7)^2 + 0.0408 Ar} - 33.7 \qquad (6.1\text{-}2)$$

where

$$\mathrm{Re}_{mfo} = \frac{d_e U_{mfo} \rho_\ell}{\mu} \qquad (6.1\text{-}3)$$

when U_{mf} : minimum fluidization velocity in three-phase fluidize bed system (m/s)

U_{mfo} : minimum fluidization velocity of liquid-solid system (m/s)

Ar : Archimedes number, $d_p^3 \rho_\ell (\rho_s - \rho_\ell) g / \mu^2$

Re_{mfo} : Reynolds number at minimum fluidization

d_p : particle diameter (m)

ρ_ℓ : liquid density (kg/m^3)

ρ_s : solid density (kg/m^3)

μ : viscosity of fluid (kg/m•s)

Based on the above mentioned equations, the minimum fluidization velocity of the glass beads in a three-phase fluidize bed system were determined as shown in Table 6-1.

Table 6-1 Calculated minimum fluidization velocity in a three-phase fluidize bed system

U_g		U_{mfo}	U_{m_f}
(cm/min)	(x10^{3}m/s)	(x10^{3}m/s)	(x10^{3}m/s)
10	1.7	0.9	0.75
20	3.3	0.9	0.71
40	6.7	0.9	0.66

From Table 6-1, it is reasonable to imply that moving of the glass bead was a direct consequence effect of gas flow which was much higher than the minimum fluidization velocity (U_{mf}). Such flow could also give rise to the particle-particle and particle-cell interaction. When the impact forces due to particle-cell interaction were higher than the yield strength of the cells, they would become disrupted. Similarly the collision of cell and glass bead could also result in the damaged of cells. This implied mechanism was consistent with that of Heim and coworker (1999). They proposed that cells were disrupted due to the system of the external force (N) generated from the collision of grinding media and the perpendicular resultant force W in the destruction zone (Figure 6-6). Both of these forces could destroy cell walls.

Meanwhile, shear stresses were also generated in the system when bubbles were flowing in column. From Nishikawa's relation (Chisti, 2001), shear rate could be calculated by the following equation;

$$\gamma_{av} = kU_g^{a} \qquad (6.1\text{-}4)$$

when γ_{av} : average shear rate (1/s)

U_g : gas velocity (m/s)

In this equation, when gas velocity was lower than 0.04 m/s, parameters k and *a* equal 1000 and 0.5, respectively. However if gas velocity was equal to or higher than 0.04 m/s, parameters k and *a* become 5000 and 1, respectively. Based on this equation, the shear rate in this system could be calculated and then shown in Table 6-2.

Table 6-2 Estimation of shear rate

U_g		γ_{av} (1/s)
(cm/min)	($x10^3$ m/s)	
10	1.7	41.2
20	3.3	57.4
40	6.7	81.8

Table 6-2 shows that an increase in superficial gas velocity resulted in the increasing shear rate. In three-phase fluidized bed, the same trend could be assumed but its magnitude will be lower than bubble column because solid particles filled in the reactor retard the bubble motion. Rising bubbles can induce the surrounding liquid flow. However, the velocities of liquid were naturally slower than that of the bubbles. Thus, momentum transfer takes place and leads to shear stresses in the surrounding liquid. Therefore cells, which were arrested near medium-bubble interface, would be torn by shear stress so that cell wall was damaged and led to the disruption of cells. (Bavarian et al; 1991)

Regarding to the experimental results, the lowest superficial gas velocity of 10 cm/min interestingly provided the highest percentage of cell disruption. This could be implied as grinding due to collision from glass beads became predominate factor. It should be noted that the lowest superficial gas velocity gave the smallest shear stress. With higher superficial gas velocity, solid bed would become more fluidized then the distance among glass beads would become expanded. Therefore the collision between glass beads would become less. Consequently, probability of cell grinding became lower despite the increasing shear stress. However the highest superficial gas velocity of 40 cm/min could provide slightly increased cell ruptured percentage due to the increasing shear stress in the liquid suspension, which could compensate the decreasing collision.

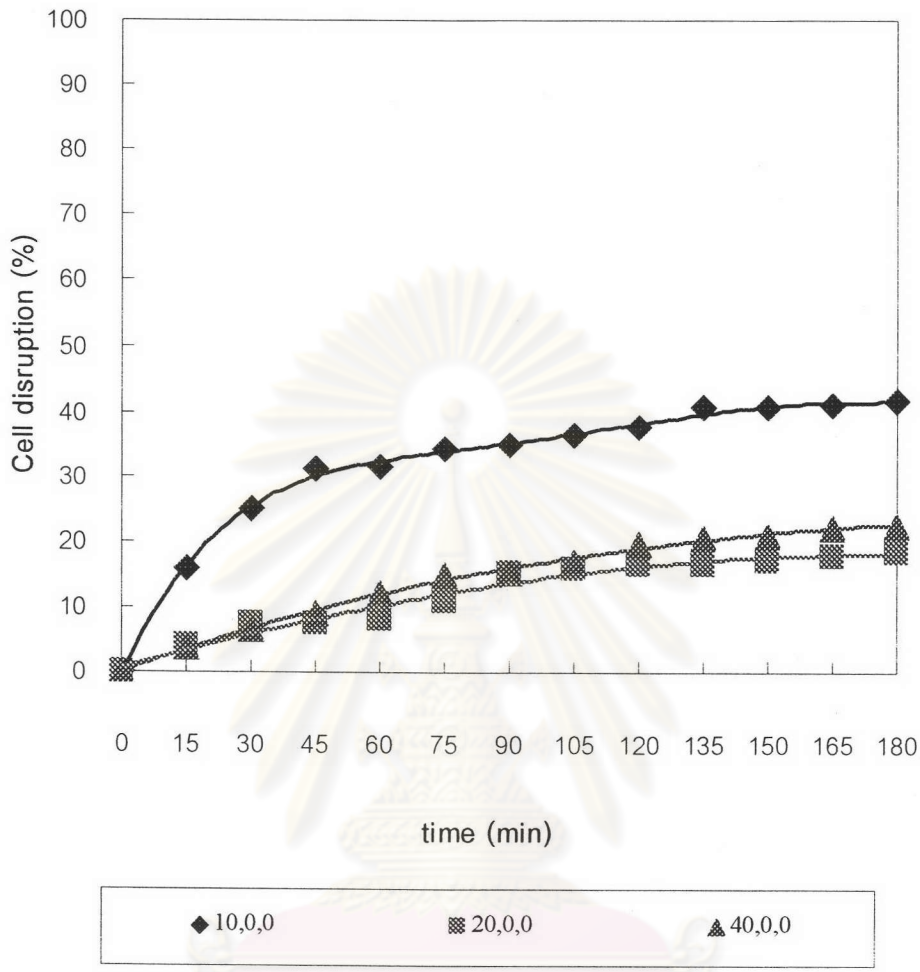

Figure 6-1. Percentage of *Chlorella ellipsoidea* cells disruption at various superficial gas velocities.

U_g = 10, 20, 40 cm/min

U_l = 0 cm/min

N = 0 rpm

(U_g,U_l,N)

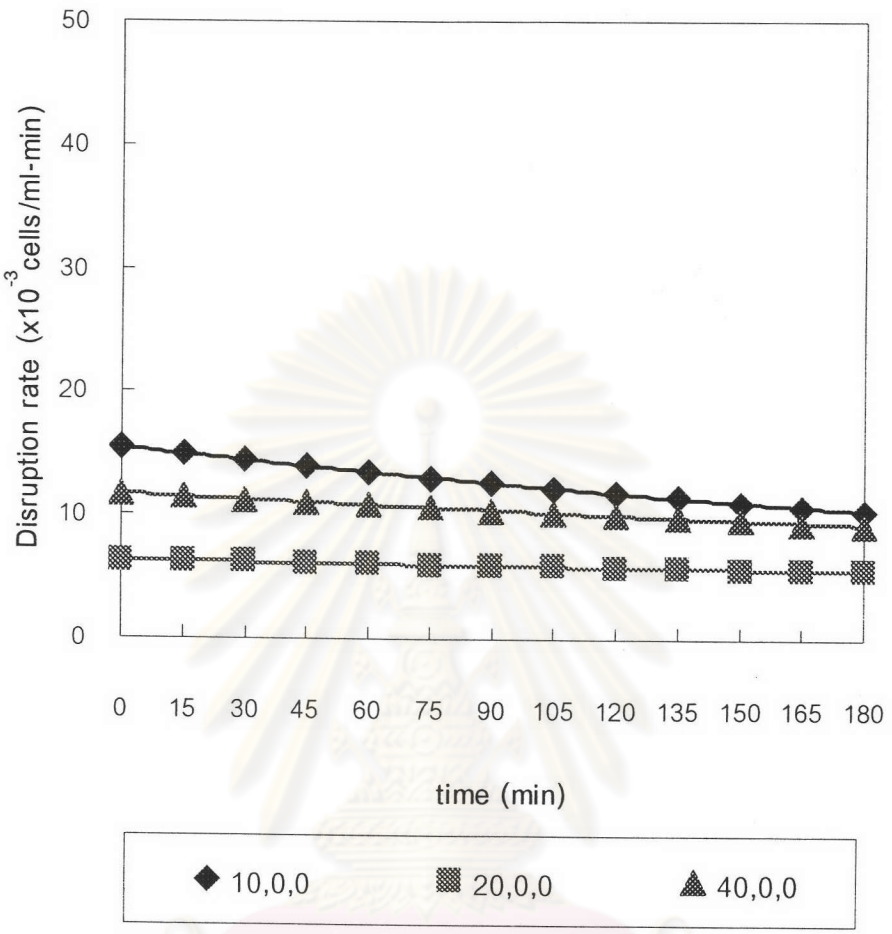

Figure 6-2. Rate of *Chlorella ellipsoidea* cells disruption at various superficial gas velocities.

U_g = 10, 20, 40 cm/min

U_l = 0 cm/min

N = 0 rpm

(U_g,U_l,N)

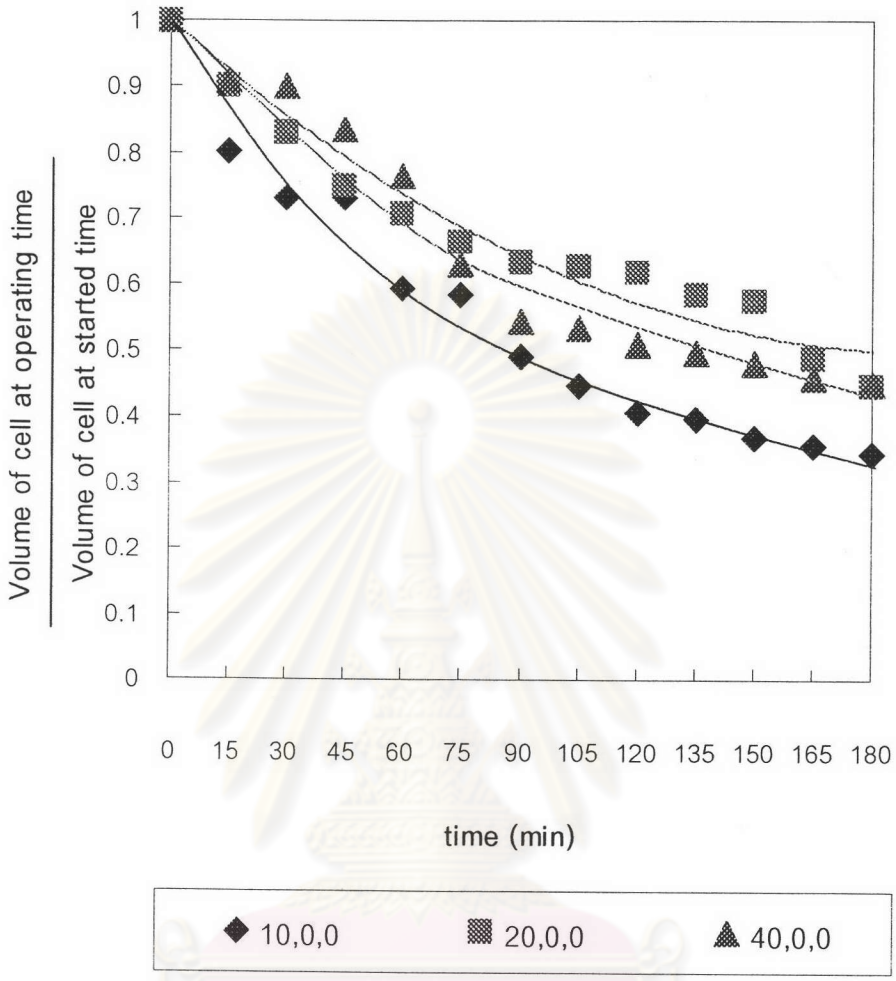

Figure 6-3. Ratio of volume of *Chlorella ellipsoidea* cells measured between various operating time and starting time at various superficial gas velocities.

U_g = 10, 20, 40 cm/min

U_l = 0 cm/min

N = 0 rpm

(U_g,U_l,N)

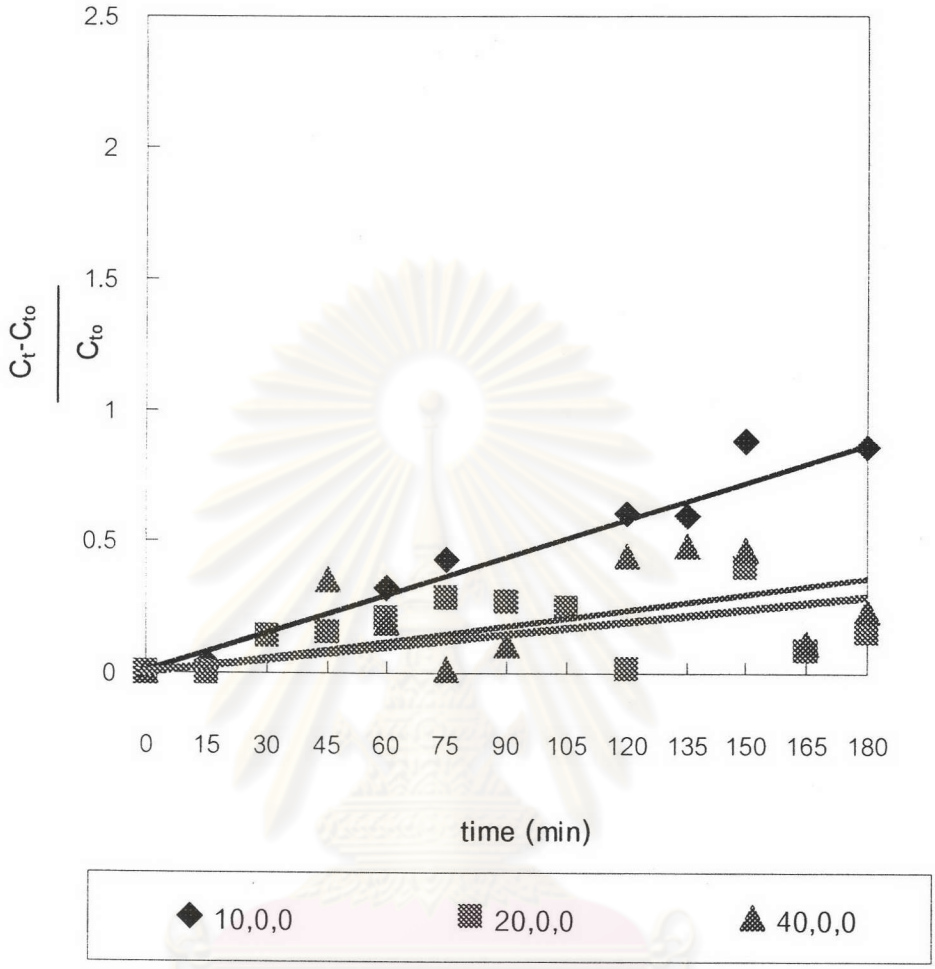

Figure 6-4. Ratio of increasing Chlorophyll A of *Chlorella ellipsoidea* cellsbetween operating time and starting time at various superficial gas velocities.

U_g = 10, 20, 40 cm/min

U_l = 0 cm/min

N = 0 rpm

(U_g,U_l,N)

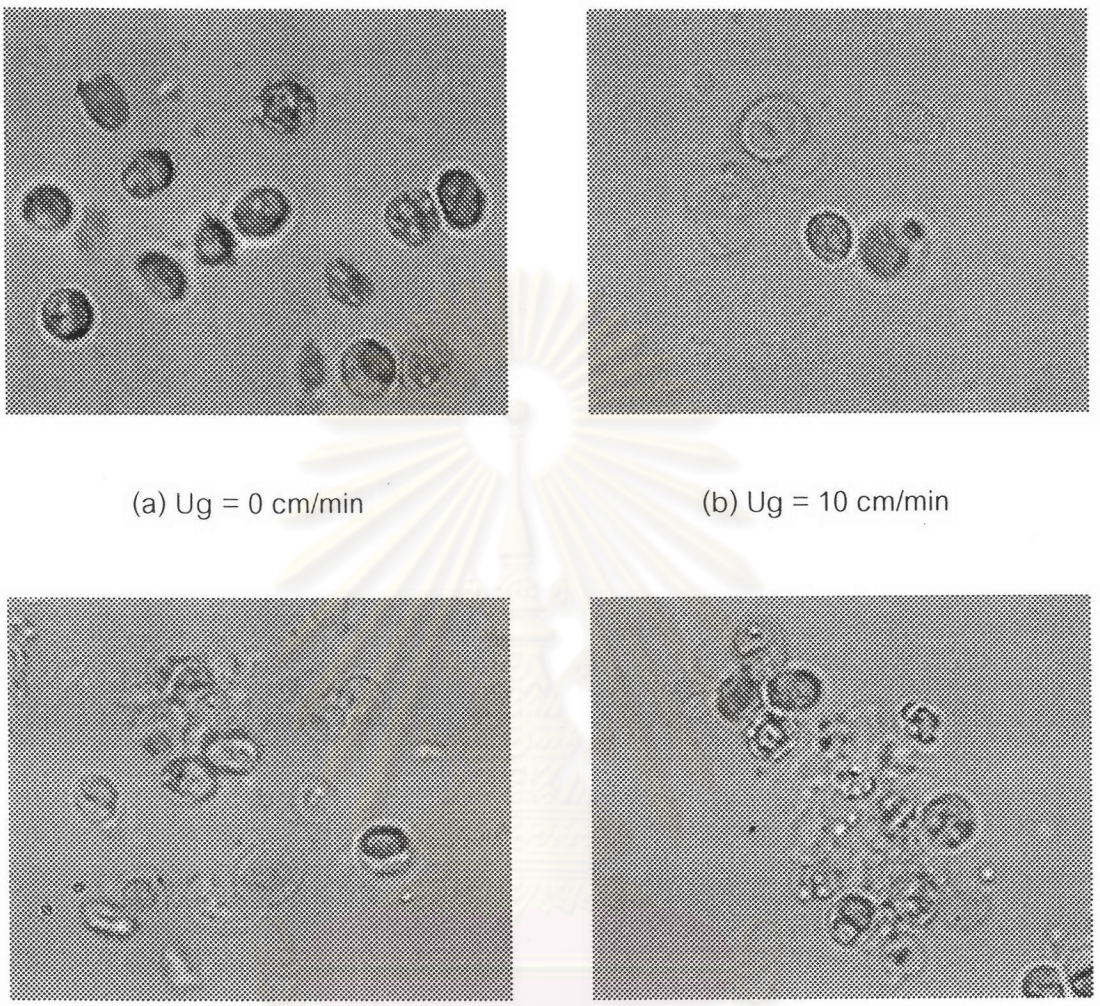

(a) Ug = 0 cm/min

(b) Ug = 10 cm/min

(c) Ug = 20 cm/min

(d) Ug = 40 cm/min

Figure 6-5. Morphology of *Chlorella ellipsoidea* (x 1000) at various superficial gas velocities

U_g = 10, 20, 40 cm/min

U_l = 0 cm/min

N = 0 rpm

(U_g,U_l,N)

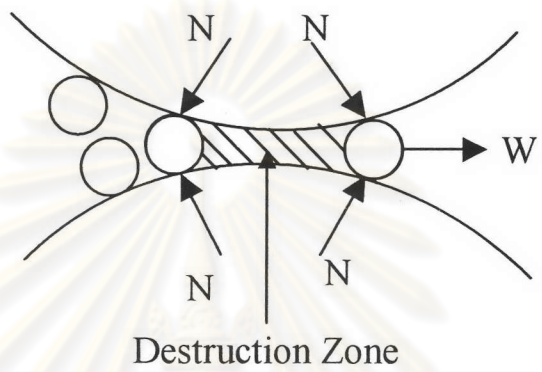

Figure 6-6. The phenomena of grinding in breaking zone

(Redrawn from Heim et al; 1999)

6.1.2 Effect of Superficial Liquid Velocity

Effect of various superficial liquid velocities had been investigated experimentally at a constant superficial gas velocity and agitating speed of 0 cm/min and 0 rpm respectively.

Figure 6-7 shows percentage of cell disruption at various superficial liquid velocities, exhibiting the highest disruption percentage of 31.5% at 10 cm/min. The percentages of cell disruption declined to 14.9% at 20 cm/min. However with increasing superficial liquid velocity to 40 cm/min, the disruption becomes slightly increased to 19.3%.

Accordingly, the results of rate of cell disruption (Figure 6-8), alteration of cell volume with respect to the operating time (Figure 6-9), amount of Chlorophyll A (Figue 6-10) and photograph of cell morphology (Figure 6-11) exhibit the consistent trends.

Cell disruption took place when the liquid was flowing in the column. Shear rate was generated by liquid flowing. However shear stress with the absence of glass beads had a little effect on cell ruptured (only 1.7%) even at the liquid flow rate of 40 cm/min (Figure 6-7). With the presence of glass bead, under the same operating conditions, the disrupting percentage can be increased up to 19.3%. These lead to an implication that shear stress from liquid flow was inadequate to damage cell. On the other hand, interaction between glass beads with assistance of liquid flow could help increase the cell breakage. Liquid flow results in motion of glass bead particle and collision between glass bead and cells. As a consequence, microalgal cells will experience the liquid shear and collision with glass beads, which lead to the disruption.

From Figure 6-8, at superficial liquid velocity of 10 cm/min, an optimal percentage of cell disruption of 38.5% could be observed. A further increase in superficial liquid velocity to 20 and 40 cm/min resulted in the disruption percentage of

14.9 and 19.3, respectively. This could be implied that despite of the increasing shear, a decrease in contact time among cells and glass beads due to the increase in superficial liquid velocity would play on important role in microalgal cell disruption. Although the increase in superficial liquid velocity to 40 cm/min could provide a slight increase in cell disruption percentage to 19.3%, it could be clearly seen that the disruption percentage is much lower than that of 10 cm/min by which the contact time could be assumed much longer.

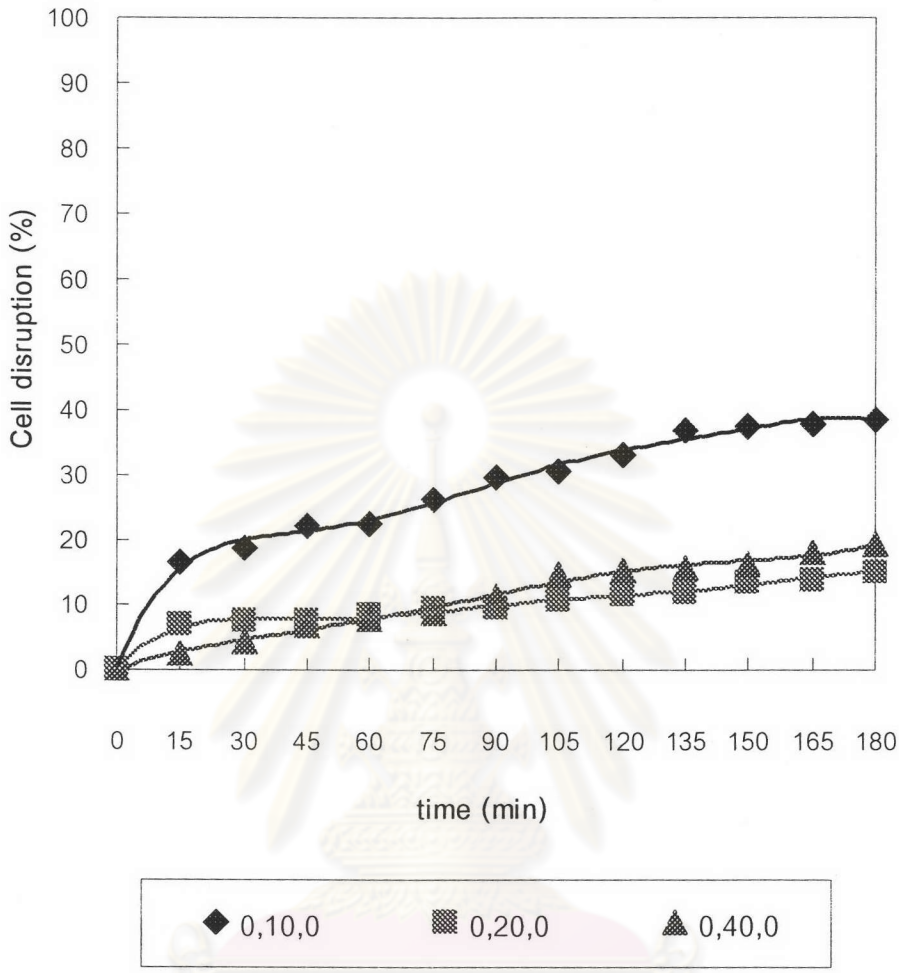

Figure 6-7. Percentage of *Chlorella ellipsoidea* cells disruption at various superficial liquid velocities.

U_g = 0 cm/min

U_l = 10, 20, 40 cm/min

N = 0 rpm

(U_g,U_l,N)

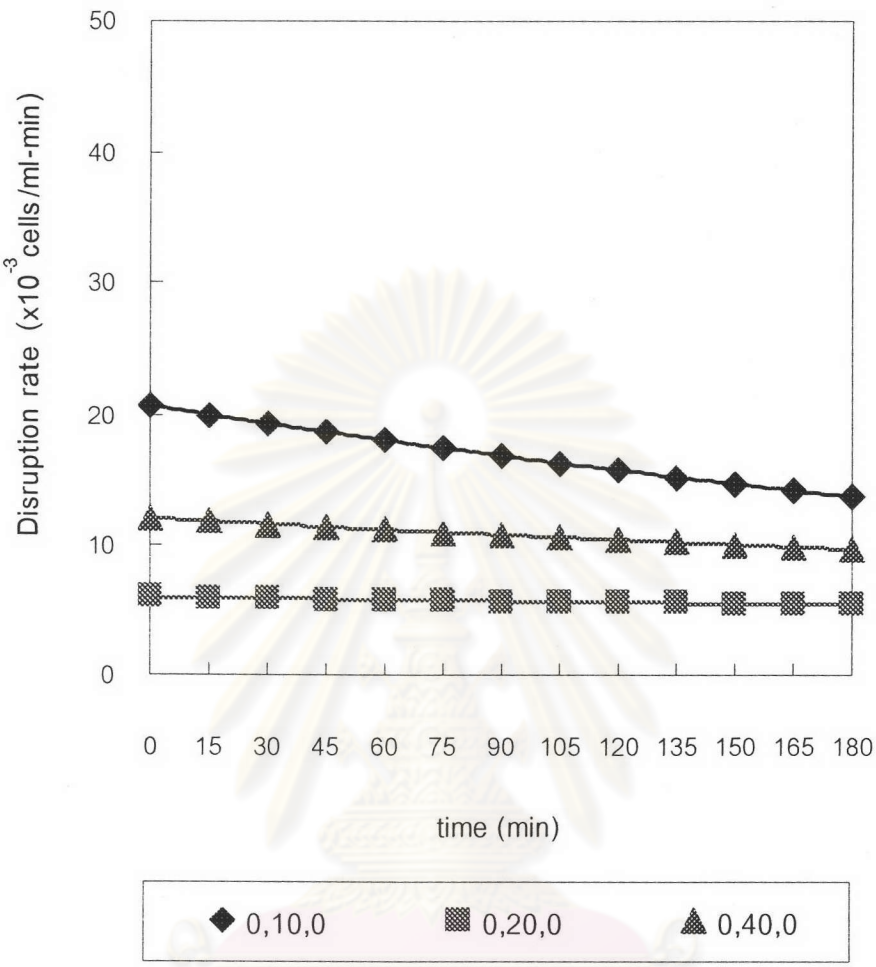

Figure 6-8. Rate of *Chlorella ellipsoidea* cells disruption at various superficial liquid velocities

U_g = 0 cm/min

U_l = 10, 20, 40 cm/min

N = 0 rpm

(U_g,U_l,N)

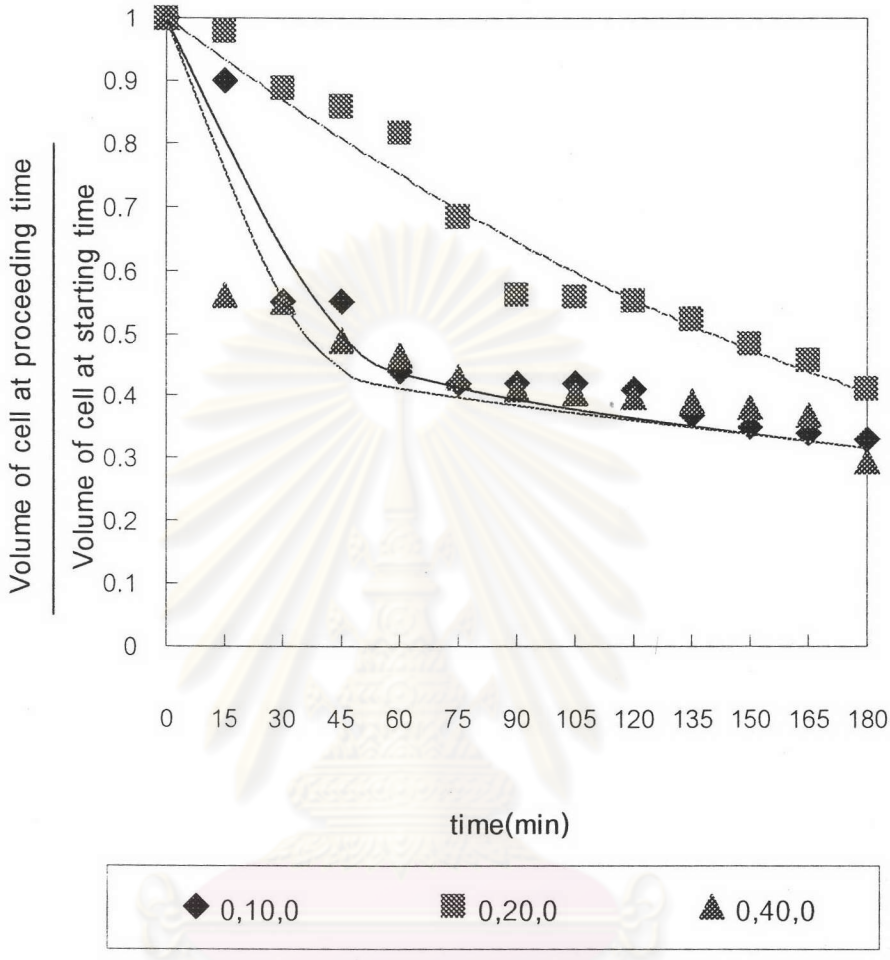

Figure 6-9. Ratio of volume of *Chlorella ellipsoidea* cells measured between various operating time and starting time at various superficial liquid velocities

U_g = 0 cm/min

U_l = 10, 20, 40 cm/min

N = 0 rpm

(U_g,U_l,N)

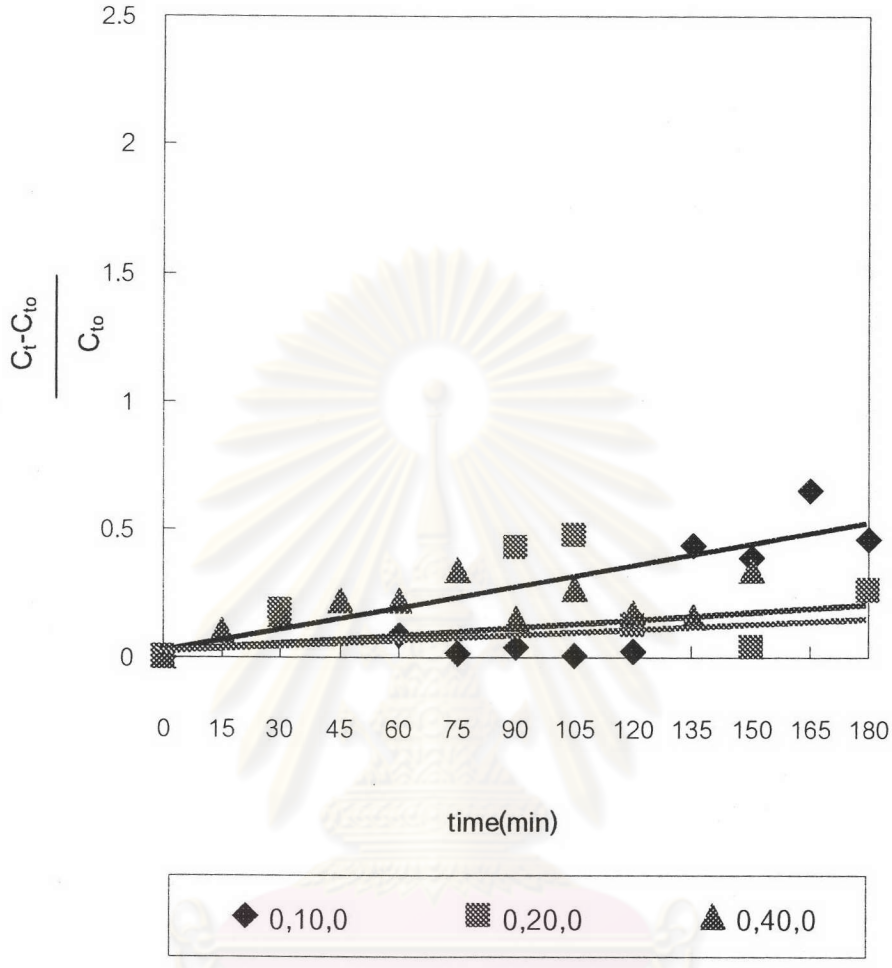

Figure 6-10. Ratio of increasing Chlorophyll A of *Chlorella ellipsoidea* cells between operating time and starting time at various superficial liquid velocities

U_g = 0 cm/min

U_l = 10, 20, 40 cm/min

N = 0 rpm

(U_g,U_l,N)

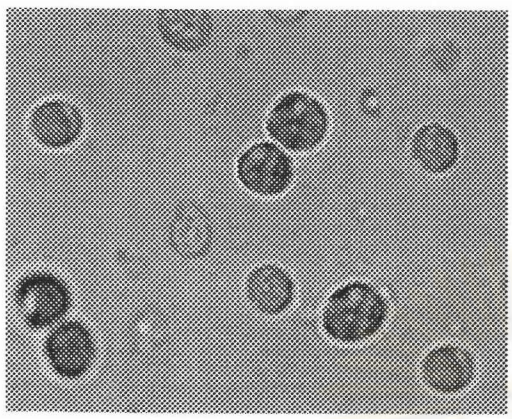

(a) U_l = 0 cm/min

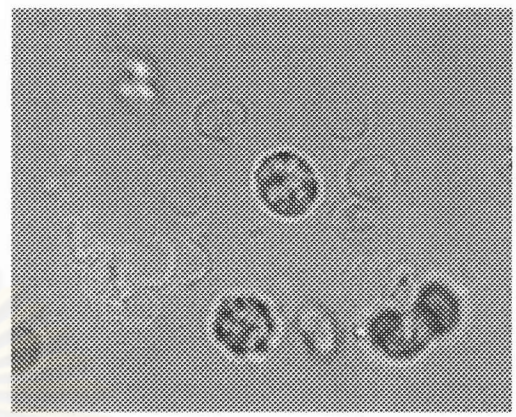

(b) U_l = 10 cm/min

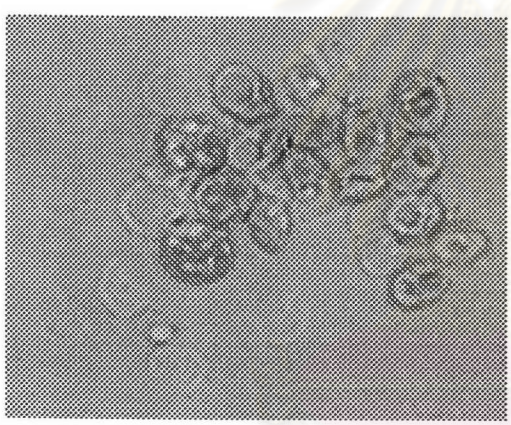

(c) U_l = 20 cm/min

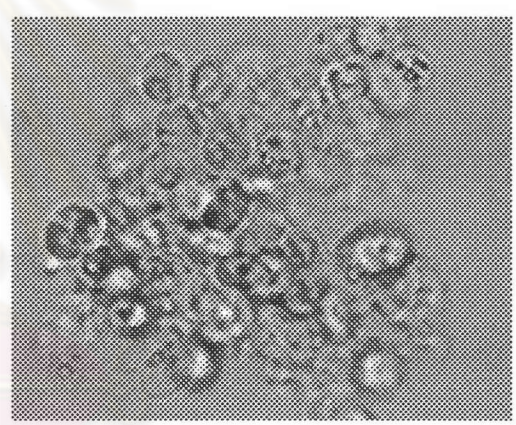

(d) U_l = 40 cm/min

Figure 6-11. Morphology of *Chlorella ellipsoidea* (x1000) at various superficial liquid velocities.

U_g = 0 cm/min

U_l = 10, 20, 40 cm/min

N = 0 rpm

(U_g,U_l,N)

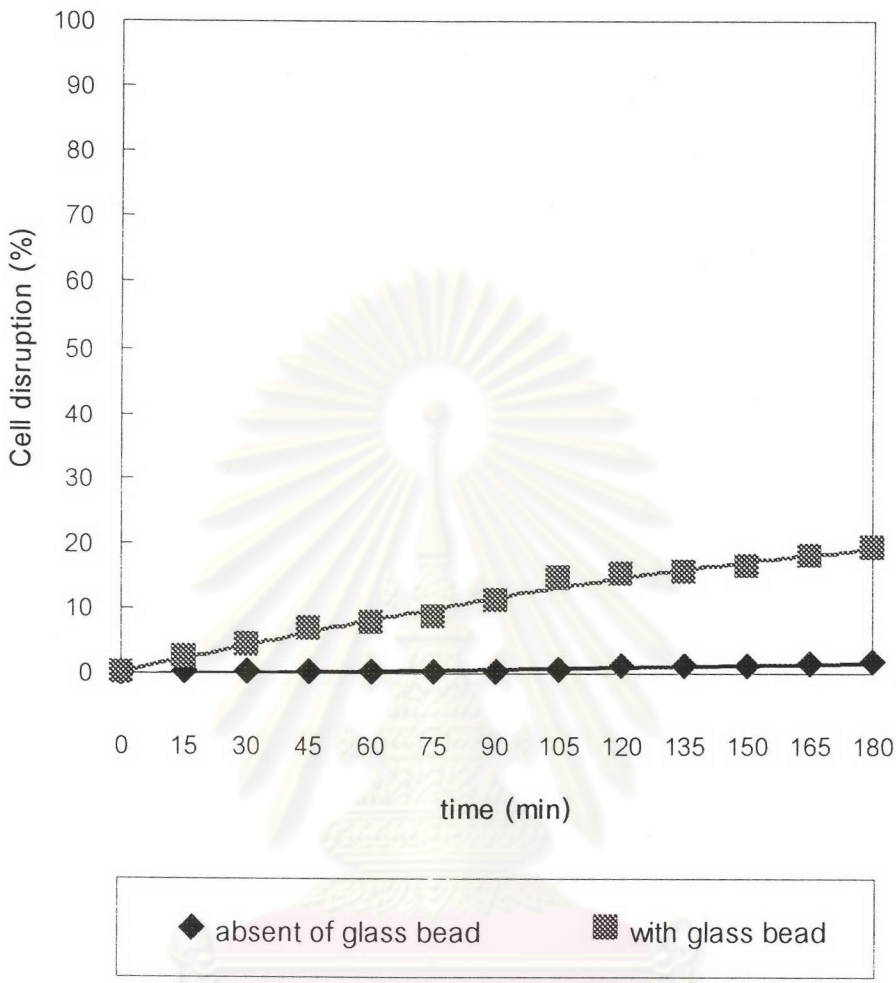

Figure 6.12. Percentage of *Chlorella ellipsoidea* cells disruption at various superficial liquid velocities

U_g = 40 cm/min

U_l = 0 cm/min

N = 0 rpm

(U_g,U_l,N)

6.1.3 Effect of Agitation

The effect of the agitation was investigated in batch operating conditions. The experiments were conducted by varying the agitation speed as 500, 1500, 2000 and 3000 rpm without the superficial gas and liquid velocity. Consequently, cell disruption can be considered by 2 mechanisms: the cell disruption generated from the tangential force generated from the agitation and the impact force due to the collision glass beads.

Figure 6-13 reflects the percentage of cell disruption counted from the living cell at any times using Sidwicks-Rafter countering chamber. It is cleanly seen that an increase in the agitation speed could provide the increasing cell disruption. Moreover, the result were confirmed by rate of cell disruption (Figure 6-14), cell size from ratio between cell volumn at operating time and starting time (Figure 6-15) and Chlorophyll A released (Figure 6-16). Similarly, consideration of cell morphology observed at the magnification of 1000 in Figure 6-17 could lead to the consistent trend. It shows cell debris when the agitation was employed.

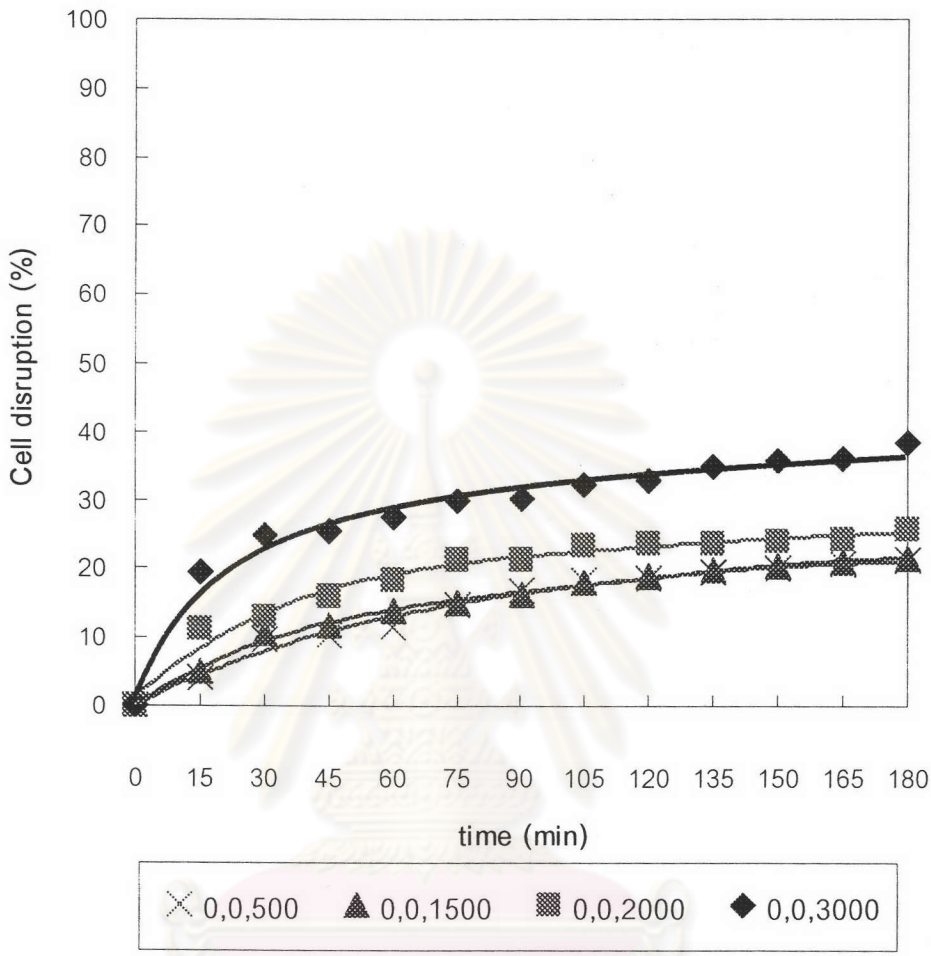

Figure 6-13. Percentage of *Chlorella ellipsoidea* cells disruption at various agitation speeds

U_g = 0 cm/min

U_l = 0 cm/min

N = 500,1500, 2000 and 3000 rpm

(U_g,U_l,N)

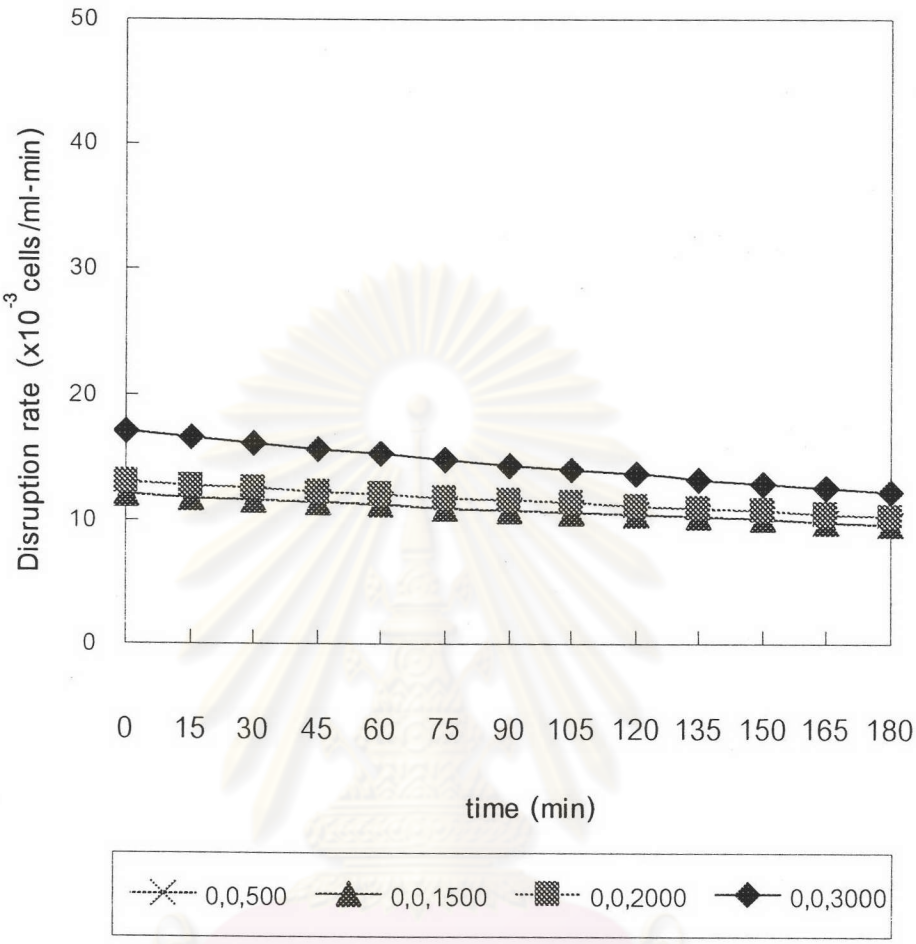

Figure 6-14. Rate of *Chlorella ellipsoidea* cells disruption at various agitation speeds

U_g = 0 cm/min

U_l = 0 cm/min

N = 500,1500, 2000 and 3000 rpm

(U_g,U_l,N)

Regarding the experimental results of Currie et al, 1972; Shamlou et al, 1995; and Chisti, 2001 the consistent trend could be observed. The significant mechanisms of microalgal cell disruption were shear from agitation and the mobilization of glass bead.

Agitation could influence not only the flowing of fluid but also the movement of glass beads in the system (Currie et al., 1979). The collision between glass beads and cells could result in cell disruption, especially, when cells were between glass beads. Anyway, the collision between cells and others in the reactor was just one of the mechanisms for disrupting cells in the system. When the agitation velocity was increased, the liquid within the system will swift more quickly. Then, the fluctuation of velocity and tangential force inserting on the system will become more rigorous as well. Therefore, the increase in the probability of the collision and interaction between cells and glass beads will be more enhanced due to the increasing agitation velocity. These could be implied as the main reason of the increasing cell disruption rate.

Figure 6-15 shows a noticeable increase in ratio between the average volume of cell at any times and that of starting time, which in turn could confirm the cell disruption taking place in the system. It revealed that the longer the experimental time, the more the big cells were demolished.

The ratio between the rising Chlorophyll A at any operating times and that of starting time when applying the agitation into the system was shown in Figure 6-16. More Chlorophyll A was released when the longer operating time was considered.

The morphology of cells under microscopic observation at the magnification of 1000 supports the grinding effect of glass beads at 180 minute. Figure 6-17(a) shows no cell debris at t =0, however, Figure 6-17 (b), (c) and (d) shows that more cell debris could be observed with the increasing operating time.

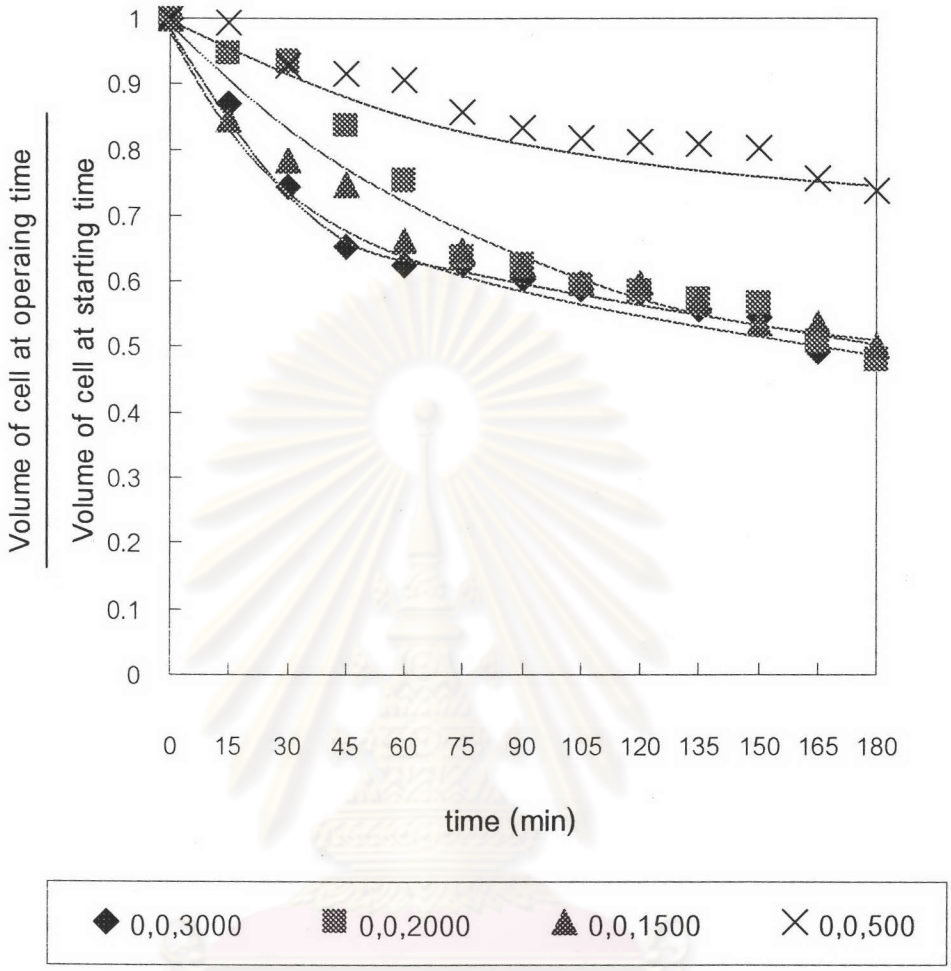

Figure 6-15. Ratio of volume of *Chlorella ellipsoidea* cells at operating time and starting time at various agitation speeds

U_g = 0 cm/min

U_l = 0 cm/min

N = 500,1500, 2000 and 3000 rpm

(U_g,U_l,N)

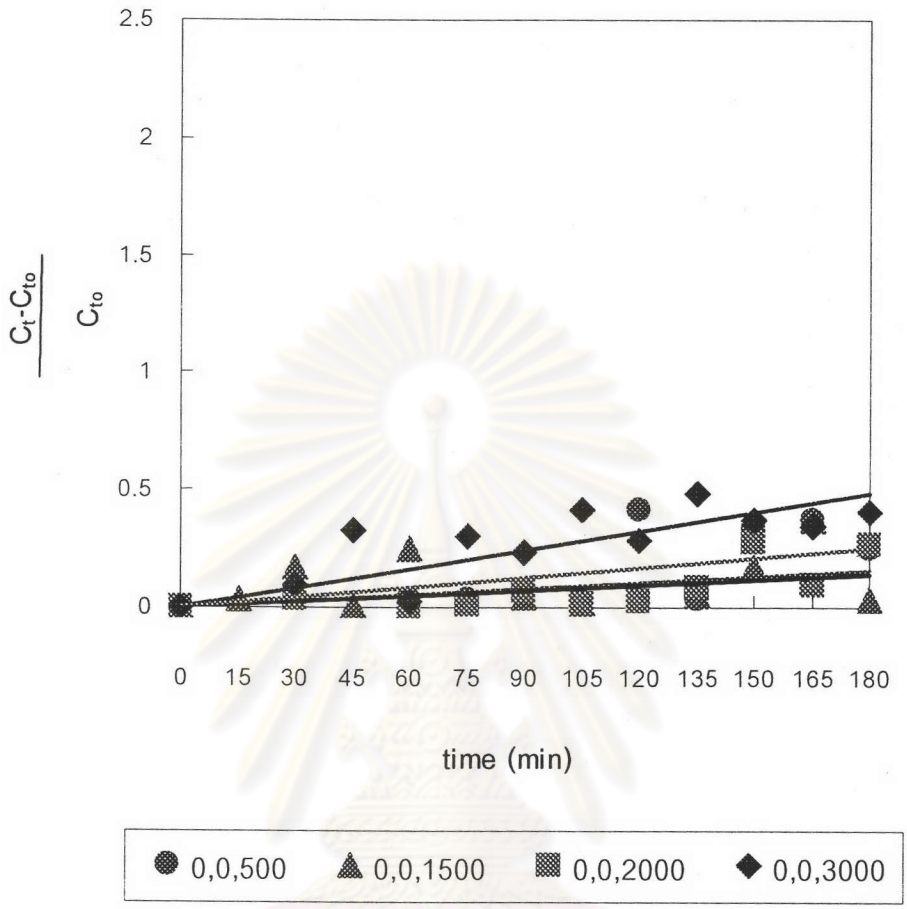

Figure 6-16. Ratio of increasing Chlorophyll A of *Chlorella ellipsoidea* cells at operating time and starting time at various agitation speeds

U_g = 0 cm/min

U_l = 0 cm/min

N = 500,1500, 2000 and 3000 rpm

(U_g,U_l,N)

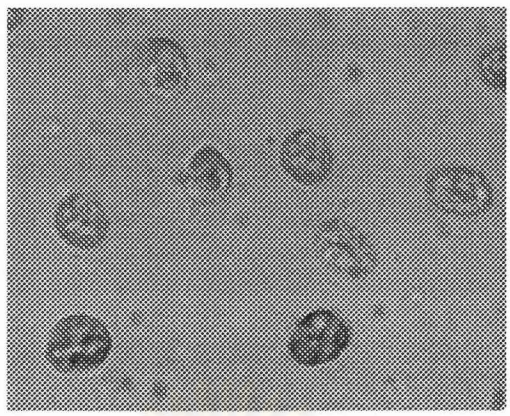

(a) 0 rpm

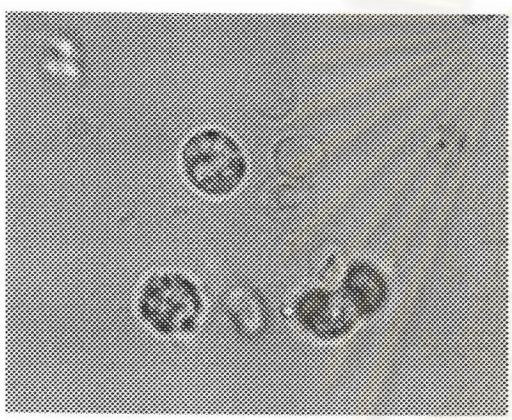

(b) 500 rpm

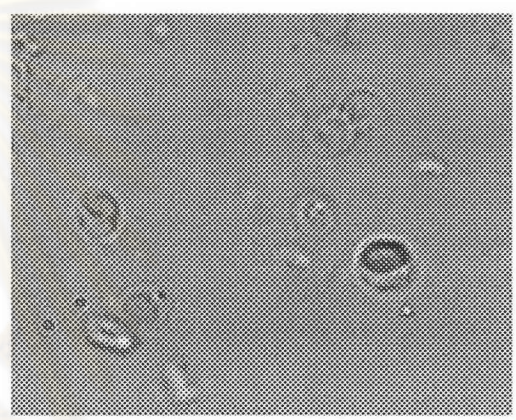

(c) 1500 rpm

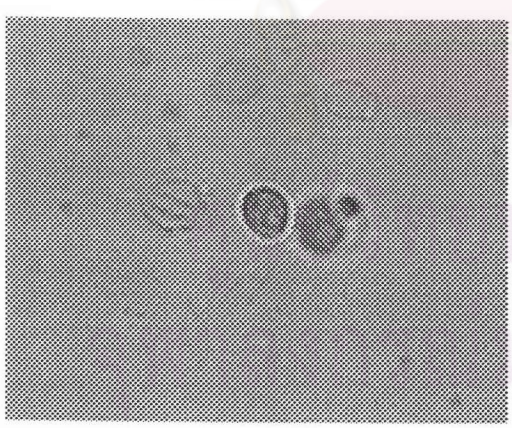

(d) 2000 rpm

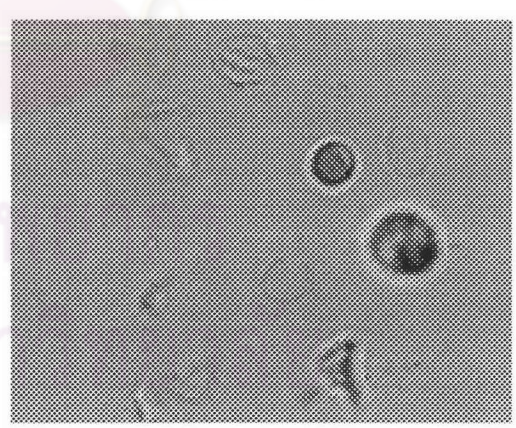

(e) 3000 rpm

Figure 6-17. Morphology of *Chlorella ellipsoidea* (x1000) at various agitation speeds

U_k = 0 cm/min

U_g = 0 cm/min

N = 500, 1500, 2000, 3000 rpm

6.1.4 Combined Effects of All Variables on Disruption of *Chlorella ellipsoidea*

Figure 6-18 shows percentage of cell disruption at various superficial gas velocities with constant superficial liquid velocity and agitating speed of 10 cm/min and 3000 rpm. Without superficial gas velocity fed into the system the percentage of cell disruption was 35.6%. However, with introducing superficial gas velocities of 10, 20, and 40 cm/min, percentage of cell disruption becomes 93.6, 60.1 and 60.4%, respectively.

It could be clearly seen that with synergetic incorporation of superficial gas and liquid velocities and agitation, the percentage of cell disrupted became tremendously increased. Motion of glass beads due to these incorporation could provide severe collision of glass bead (Chisti, 2001), in turn leading to the disruption. However excessive gas flow rate could result in bed expansion, leading to a decrease in collision between glass beads and cells.

Figure 6-19 shows a consistent trend of cell disruption rate. At the beginning, the highest disruption rate could be achieved under the optimal condition of superficial gas velocity of 10 cm/min, superficial liquid velocity of 10 cm/min and agitating speed of 3000 rpm.

Figure 6-20 shows that ratio of average cell volume measured at various operating time and starting time was influenced by introducing superficial gas and liquid velocity and agitating speed. Similarly, under the condition of superficial gas and liquid velocity of 10 cm/min and agitating speed of 3000 rpm, the average cell volume becomes drastically decreased from the beginning and than becomes almost unchanged after a certain time (approximate 75 minute) had passed.

Concentration Chlorophyll A was also measured and then shown in Figure 6-21. However, the ratio of Chlorophyll A measured at each operating time and starting time exhibits scattering behavior due to the uncertainty of measuring instrument.

More Chlorophyll A was released when longer operating time was employed. Morphology of cells at 180 minute shown in Figure 6-22 was a clear evidence for the disruption of *Chlorella ellipsoidea* cells investigated in this work.

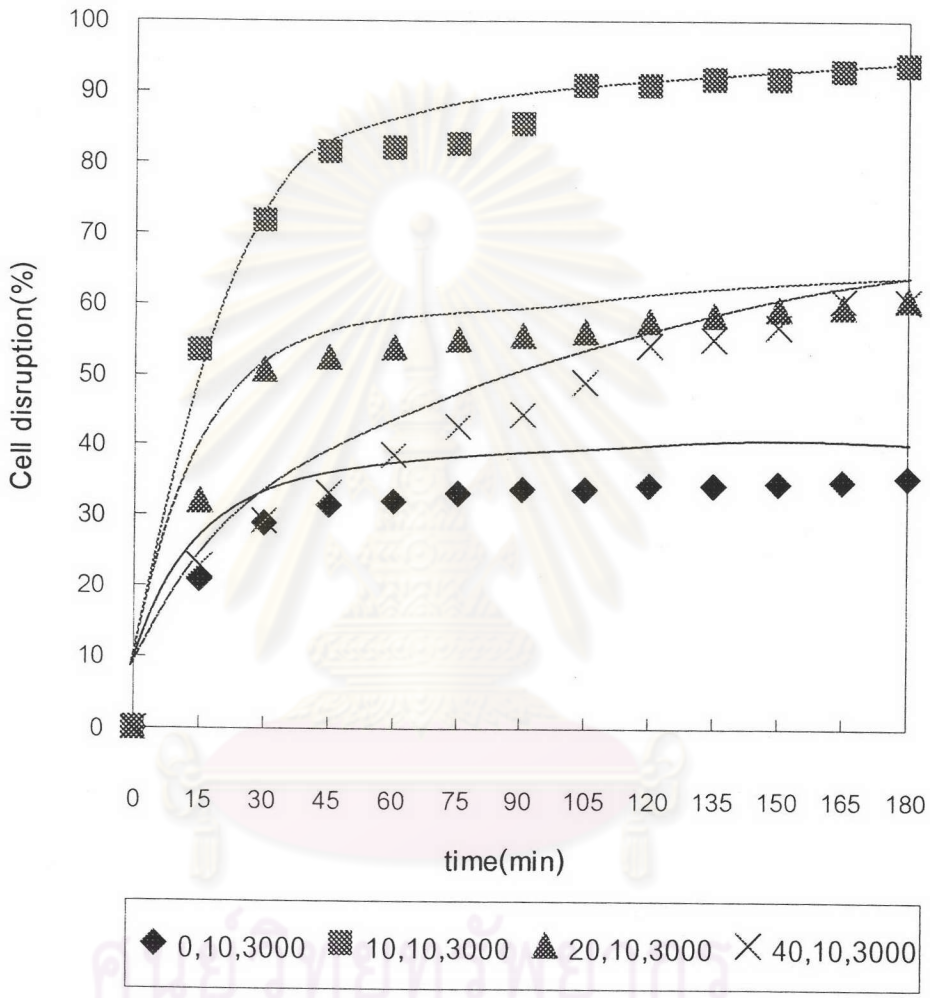

Figure 6-18. Percentage of *Chlorella ellipsoidea* cells disruption at various superficial gas velocity with constant superficial liquid velocity and agitation speed

U_g = 0, 10, 20, 40 cm/min

U_l = 10 cm/min

N = 3000 rpm

(U_g,U_l,N)

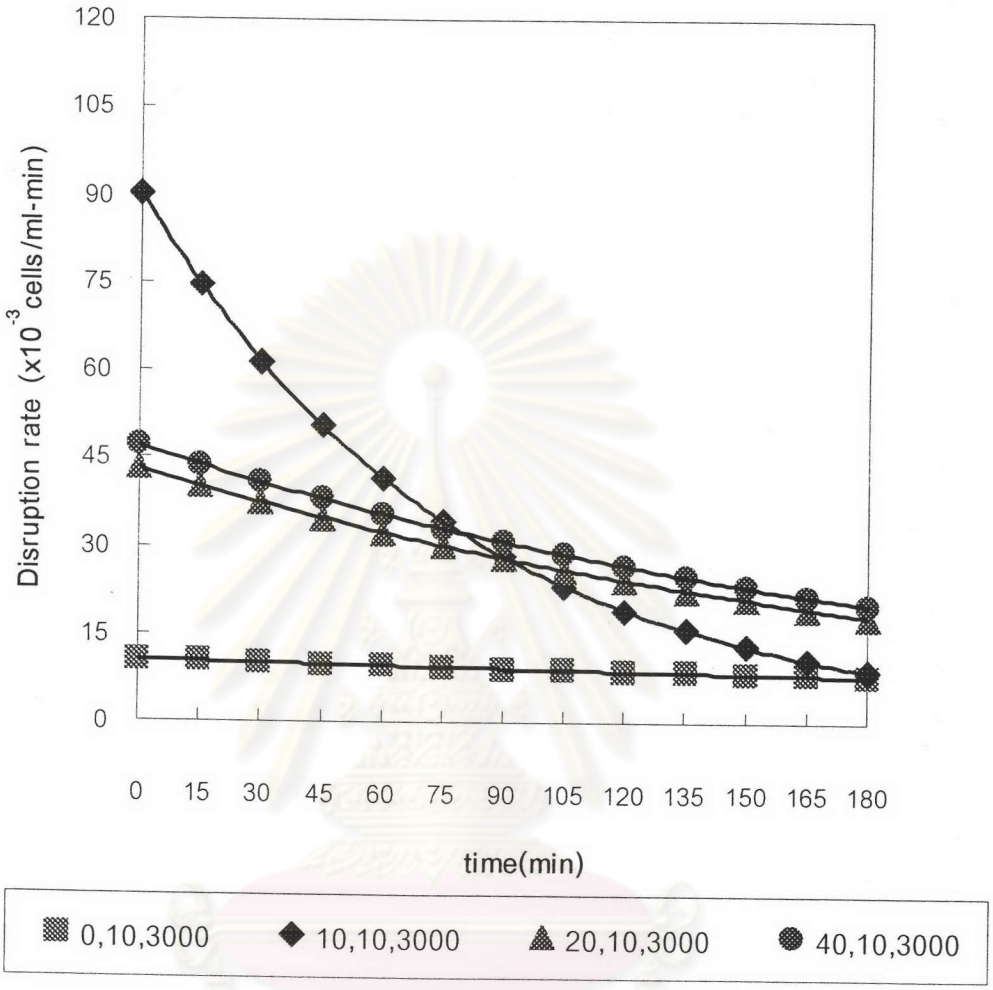

Figure 6-19. Rate of *Chlorella ellipsoidea* cells disruption at various superficial gas velocities with constant superficial liquid velocity and agitation speed

U_g = 0, 10, 20, 40 cm/min

U_l = 10 cm/min

N = 3000 rpm

(U_g,U_l,N)

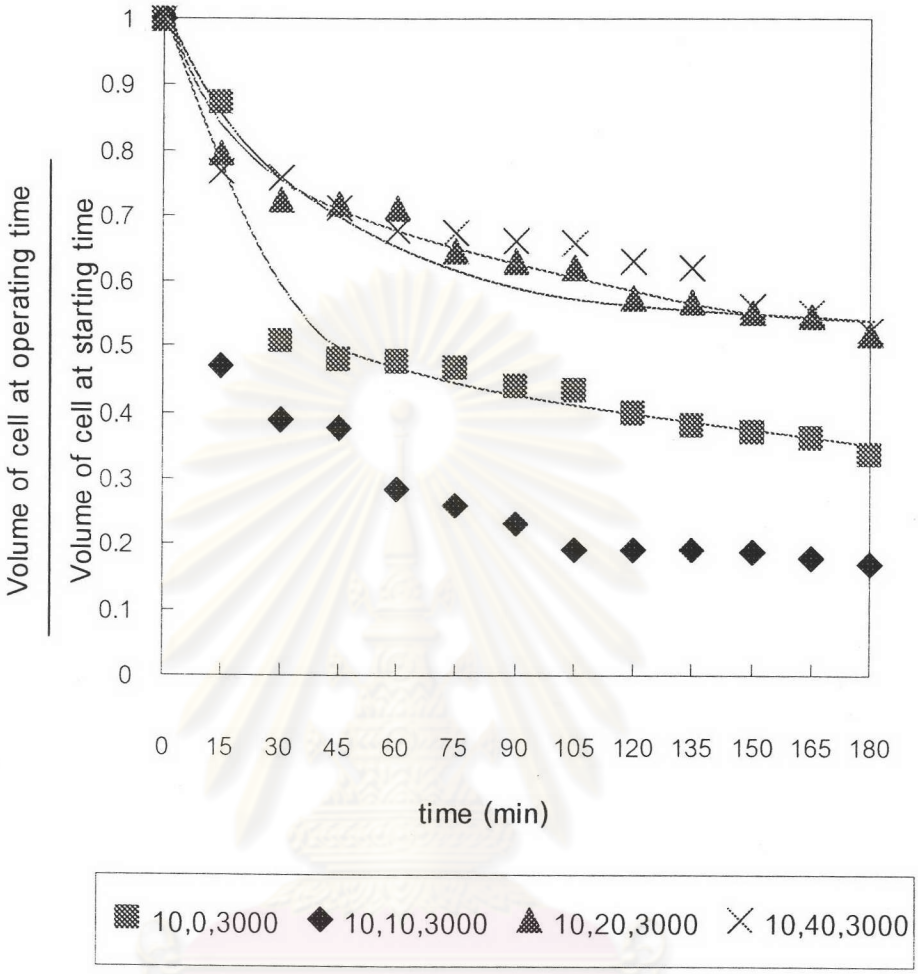

Figure 6-20. Ratio of volume of *Chlorella ellipsoidea* cells measured at various operating time and starting time at various superficial gas velocities with constant superficial liquid velocity and agitation speed.

U_g = 0, 10, 20, 40 cm/min

U_l = 10 cm/min

N = 3000 rpm

(U_g,U_l,N)

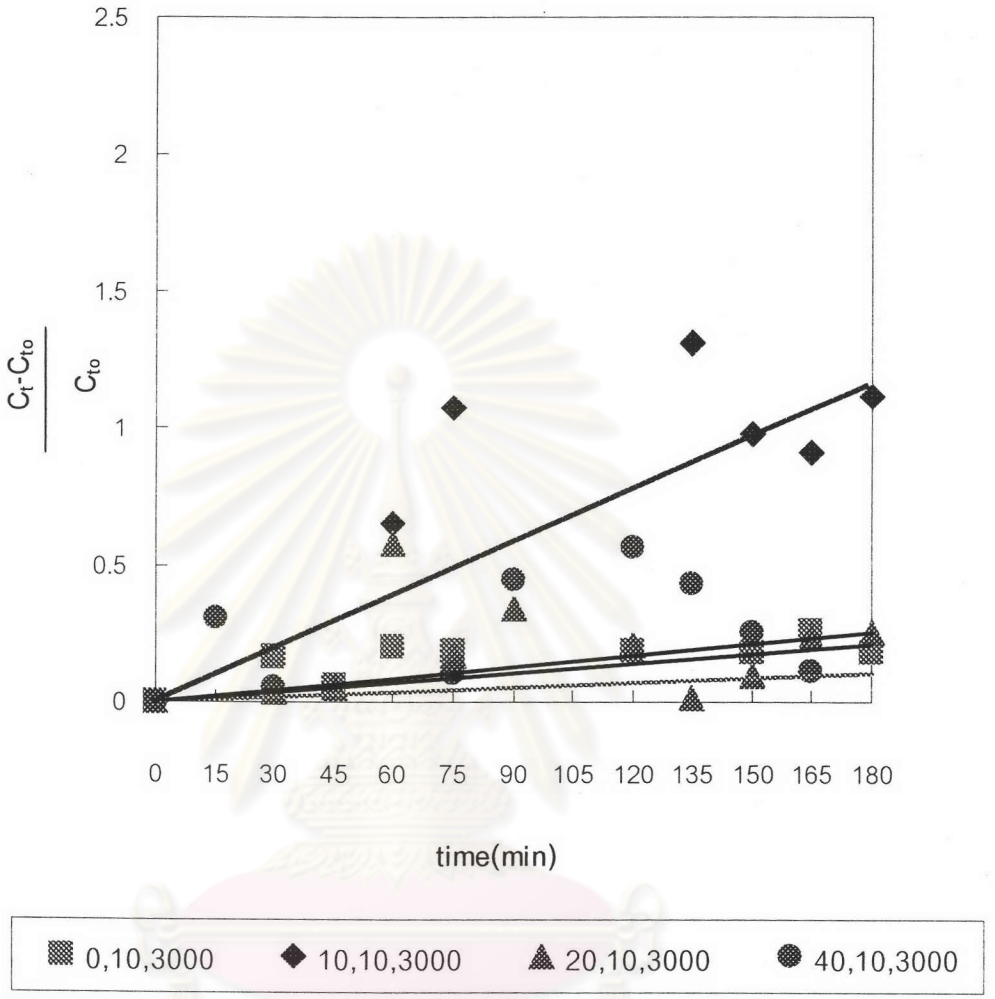

Figure 6-21. Ratio of chlorophyll a of *Chlorella ellipsoide* cells at operating time and starting time at various superficial gas velocities with constant superficial liquid velocity and agitation speed.

U_g = 0, 10, 20, 40 cm/min

U_l = 10 cm/min

N = 3000 rpm

(U_g,U_l,N)

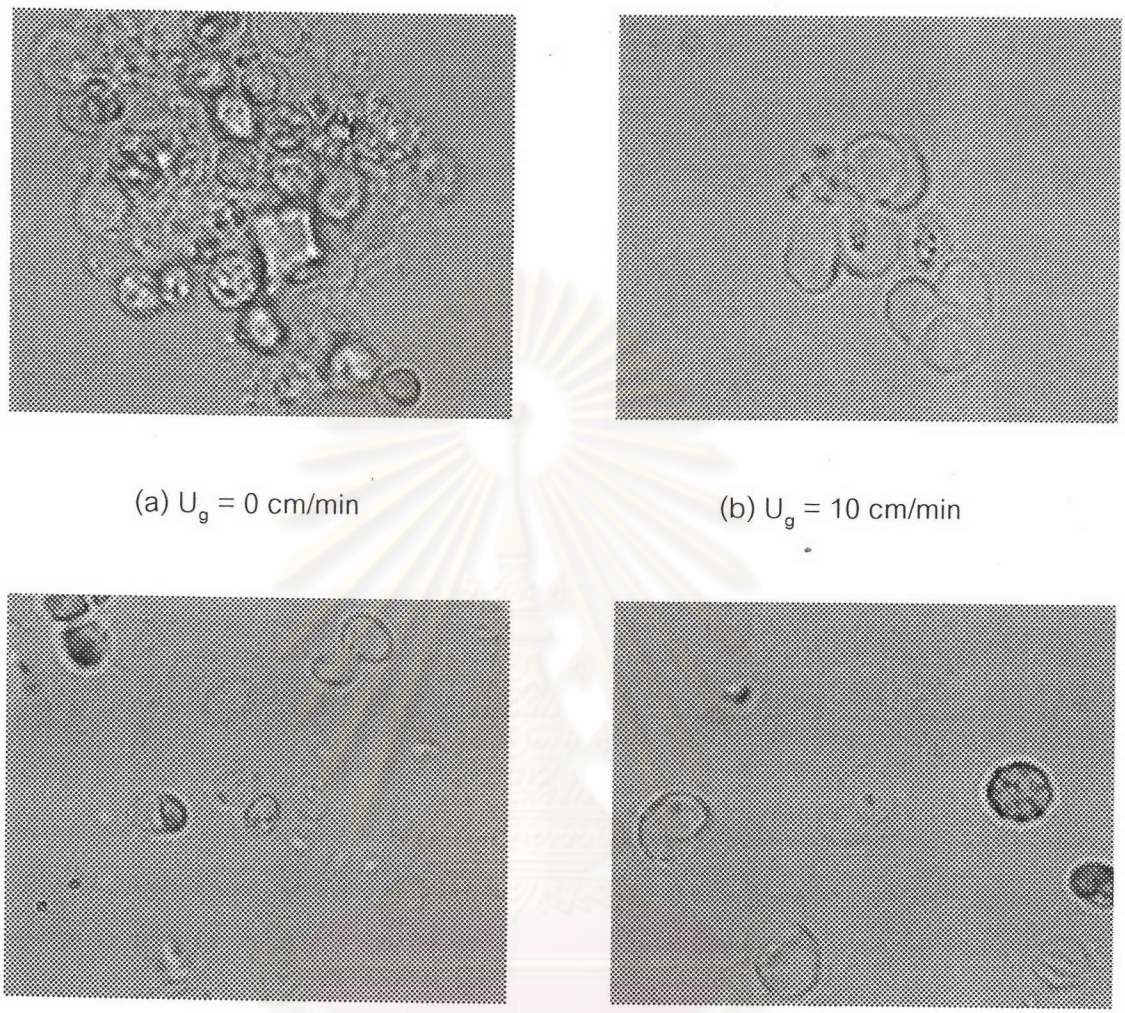

(a) U_g = 0 cm/min

(b) U_g = 10 cm/min

(c) U_g = 20 cm/min

(d) U_g = 40 cm/min

Figure 6-22. Morphology of *Chlorella ellipsoidea* (x1000) at various superficial gas velocities with constant superficial liquid velocity and agitation speed

U_g = 0, 10, 20, 40 cm/min

U_l = 10 cm/min

N = 3000 rpm

(U_g,U_l,N)

It can be seen in Figure 6-23 that percentage of cell disruption with superficial liquid velocity of 0 cm/min was 64.2%. However, when the superficial liquid velocities were fed at 10, 20, and 40 cm/min, percentage of cell disruption could be improved to 93.6, 95.7 and 93.3%, respectively. With the synergetic effects of superficial gas velocity, superficial liquid velocity and agitation, the cell disruption performance became much improved. However, an increase in the superficial liquid velocity from 10 to 40 cm/min under the employment of superficial gas velocity of 10 cm/min and agitation of 3000 rpm did not provide a significant improvement of cell disruption. This could be implied that with the increasing liquid flow the higher shear could be expected but majority of cell suspension would also pass through the column with less circulation between the core and annulus. Such counter balance would lead to a stable cell disruption performance.

Consistent trends could be observed from the data of rate of cell disruption (Figure 6-24), ratio between cell volume at operating time and starting time (Figure 6-25) and amount of released chlorophyll a (Figure 6-26). Furthermore, the microscopic observation in Figure 6-27 was again used, as an evidence of cell disruption.

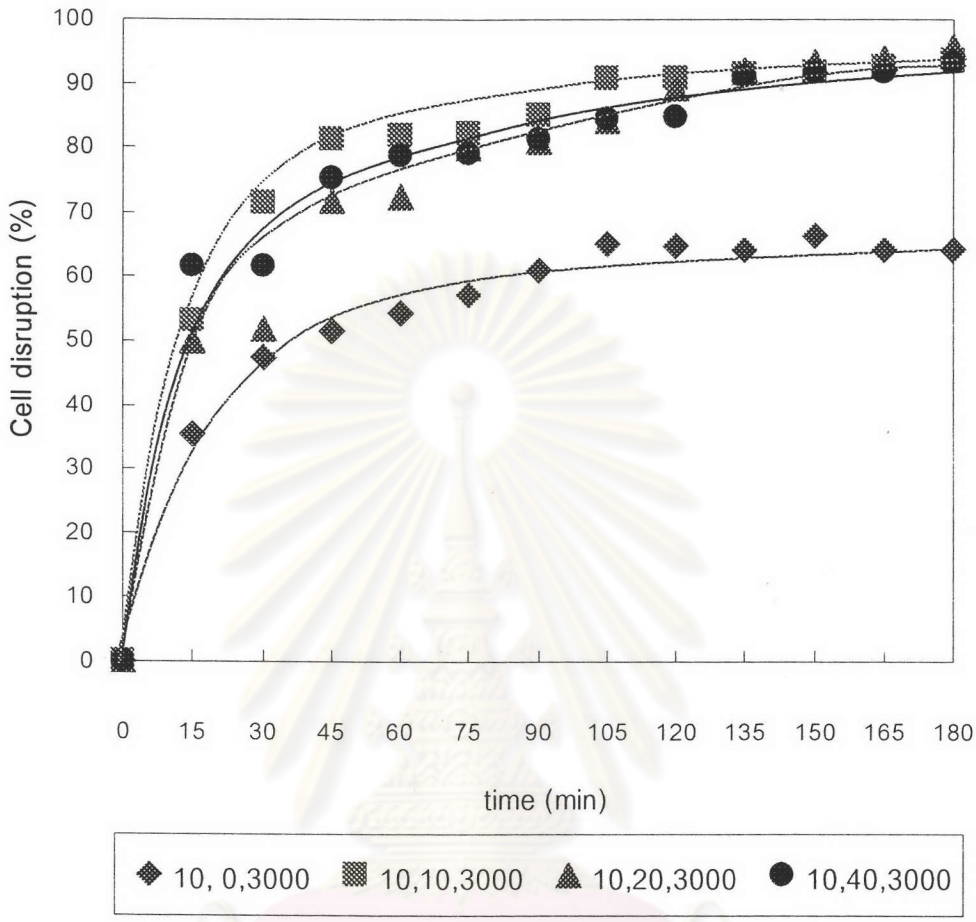

Figure 6-23. Percentage of *Chlorella ellipsoidea* cells disruption at various superficial liquid velocities with constant superficial gas velocity and agitation speed.

U_l = 0, 10, 20, 40 cm/min

U_g = 10 cm/min

N = 3000 rpm

(U_g,U_l,N)

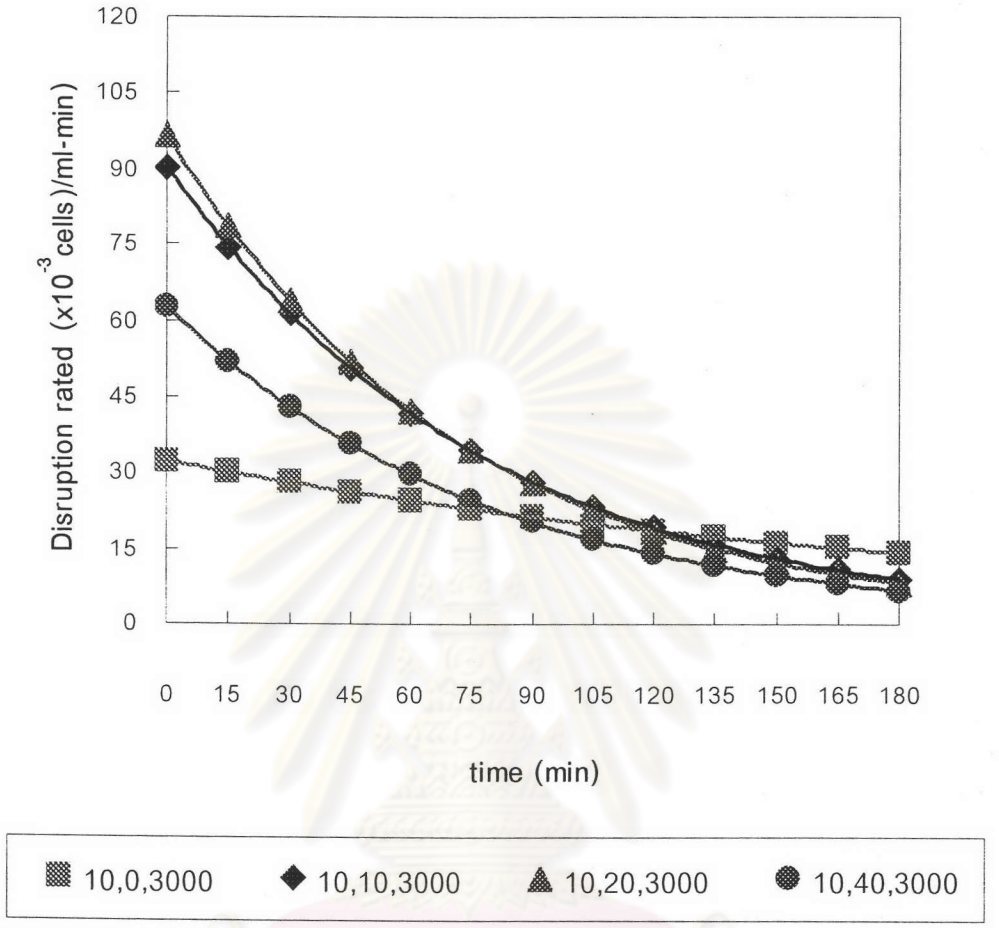

Figure 6-24. Rate of *Chlorella ellipsoidea* cells disruption at various superficial liquid velocities with constant superficial gas velocity and agitation speed.

U_g = 10 cm/min

U_l = 0, 10, 20 and 40 cm/min

N = 3000 rpm

(U_g,U_l,N)

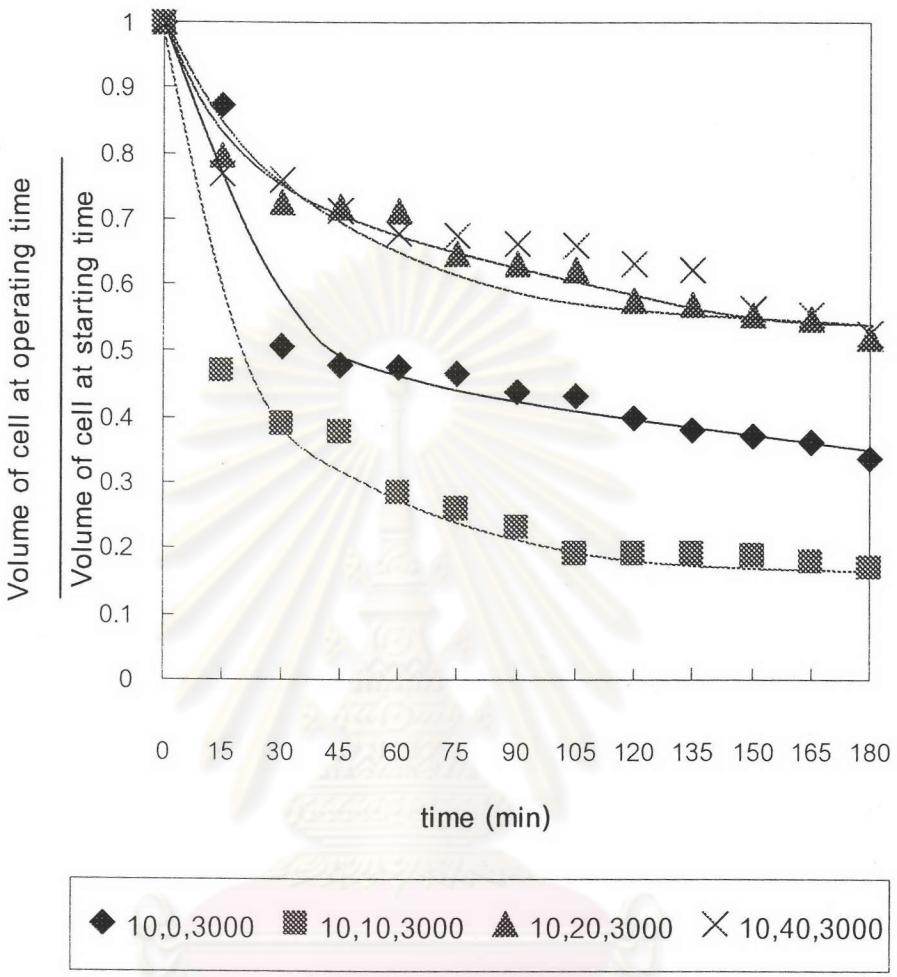

Figure 6-25. Ratio of volume of *Chlorella ellipsoidea* cells measured between various operating time and starting time at various superficial liquid velocities with constant superficial gas velocity and agitation speed.

U_g = 10 cm/min

U_l = 0, 10, 20 and 40 cm/min

N = 3000 rpm

(U_g,U_l,N)

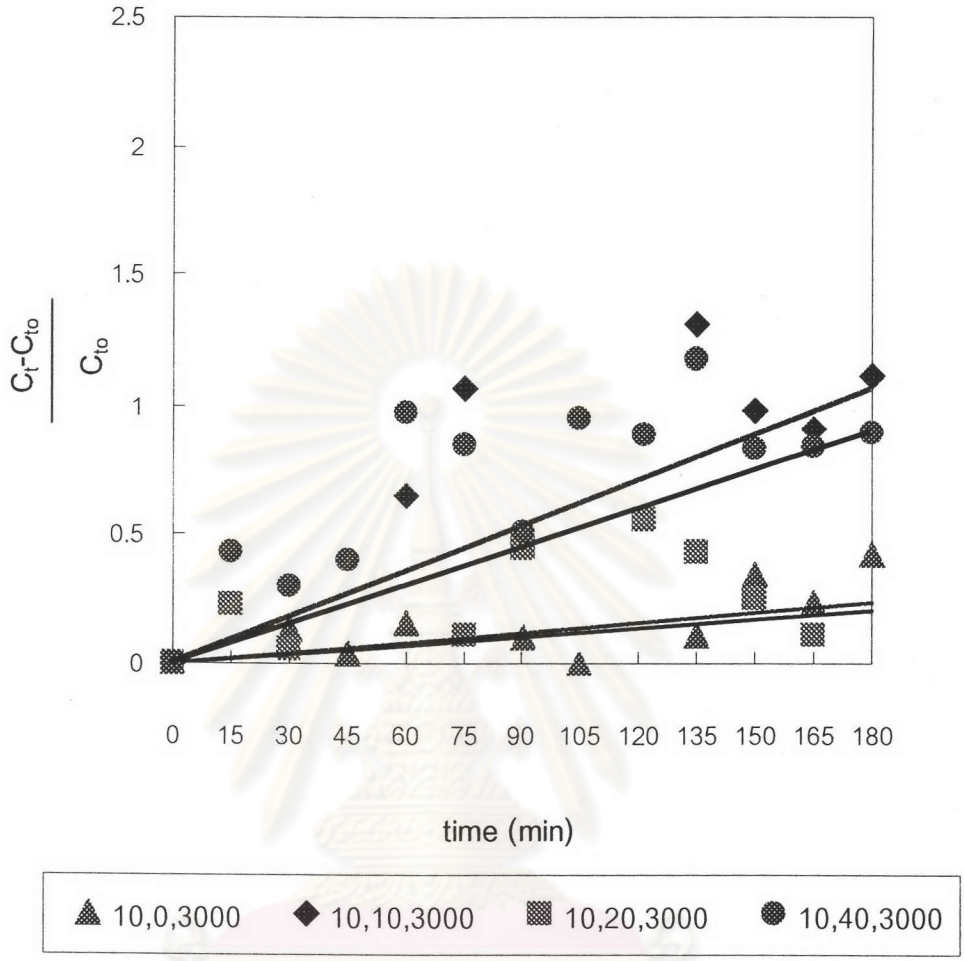

Figure 6-26. Ratio of Chlorophyll A of *Chlorella ellipsoidea* cells between operating time and starting time at various superficial liquid velocities with constant superficial gas velocity and agitation speed.

U_g = 10 cm/min

U_l = 0, 10, 20 and 40 cm/min

N = 3000 rpm

(U_g,U_l,N)

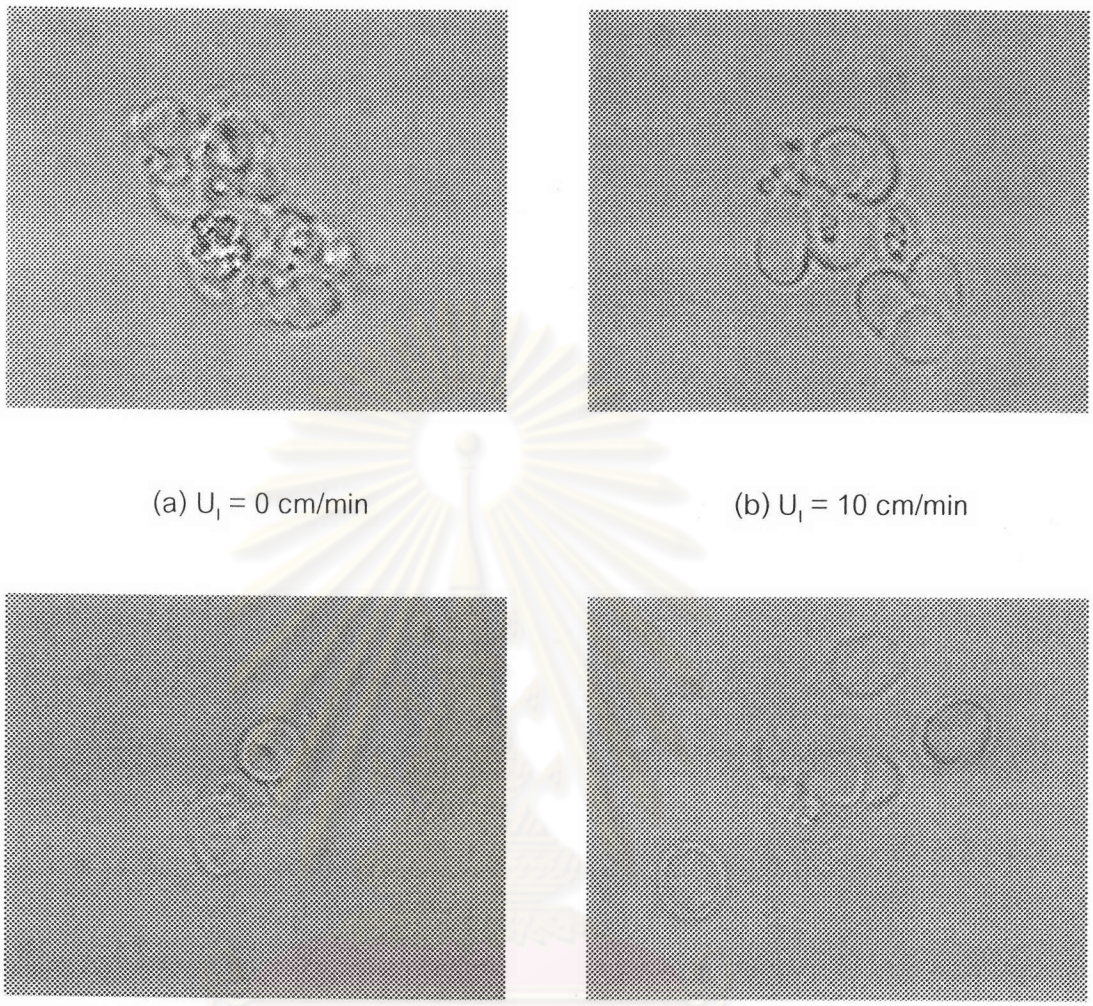

(a) U_l = 0 cm/min

(b) U_l = 10 cm/min

(c) U_l = 20 cm/min

(d) U_l = 40 cm/min

Figure 6-27. Morphology of *Chlorella ellipsoidea* (x1000) at various superficial liquid velocities with constant superficial gas velocity and agitation speed.

U_g = 0, 10, 20, 40 cm/min

U_l = 10 cm/min

N = 3000 rpm

6.2 Disruption of *Chroococcus* sp. TISTR 8623

Chroococcus sp. was also chosen to investigate in this work because it had different morphology cell wall structure compared with that of *Chlorella ellipsoidea.* However, due to the preliminary investigation, it had been found that the similar trend of cell disruption could be obtained. Therefore, only the effect of superficial gas velocity was investigated.

6.2.1 Effect of Superficial Gas Velocity on Microalgal Cell Disruption

Percentage of cell disruption was shown in Figure 6-28.The percentage become higher when longer operating time was employed. Interestingly, there was an optimal percentage of 22.3% when 10 cm/min of gas flow rate was introduced. A further increase in superficial gas velocity to 20 cm/min and 40 cm/min resulted in a decrease in percentage of cell disruption of 12.7 and 13.4%, respectively. These results were consistent with those of *Chlorella ellipsoidea.* Therefore, the similar mechanism of cell disruption may be implied for *Chroococcus* sp.

Slightly different from *Chlorella ellipsoidea*, *Chroococcus* sp. exhibited a stable disruption rate regardless of superficial gas velocities as shown in Figure 6-29. In Figure 6-30, a decrease in the average cell volume became steepest with superficial gas velocity of 10 cm/min. Consistently; Figure 6-31 shows that the steepest increase in amount of chlorophyll released from disrupted cells could be achieved with superficial gas velocity of 10 cm/min. Such disruption could also be evident in micrographs of *Chroococcus* sp. cell in Figure 6-32.

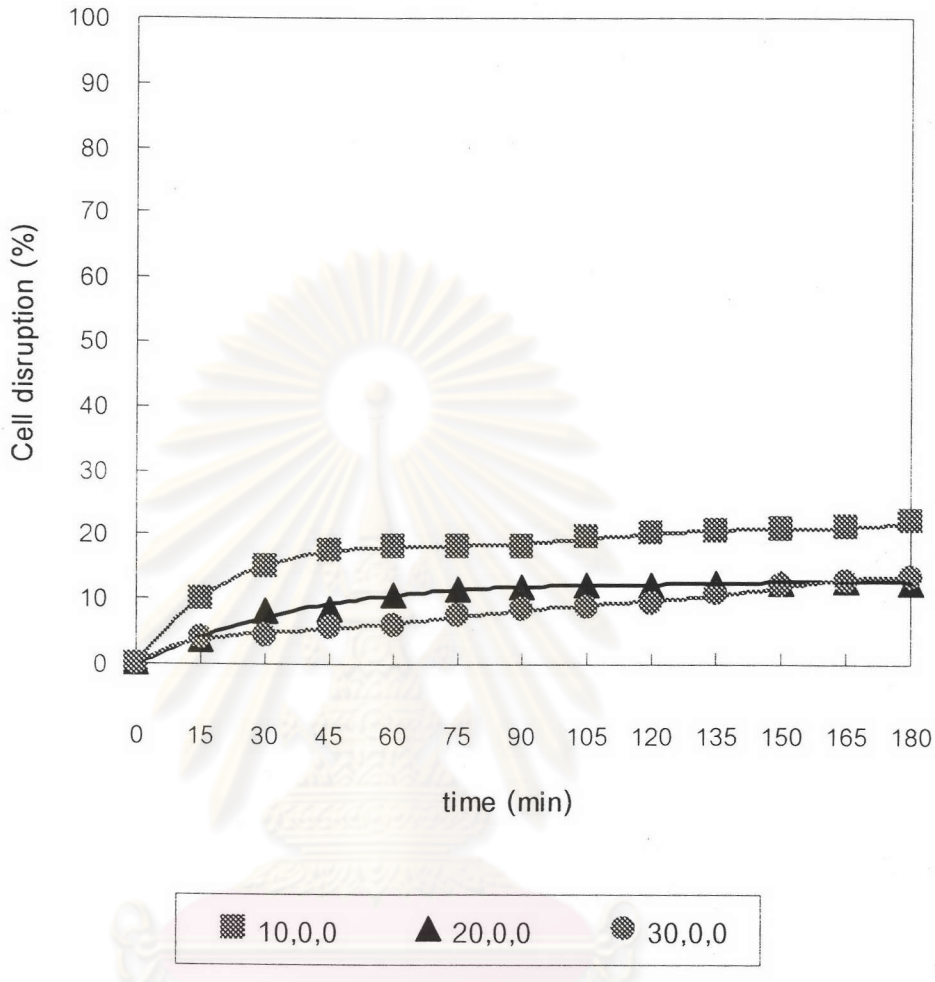

Figure 6-28. Percentage of *Chroococcus sp.* cells disruption at various superficial gas velocities

U_g = 10, 20, 40 cm/min

U_l = 0 cm/min

N = 0 rpm

(U_g,U_l,N)

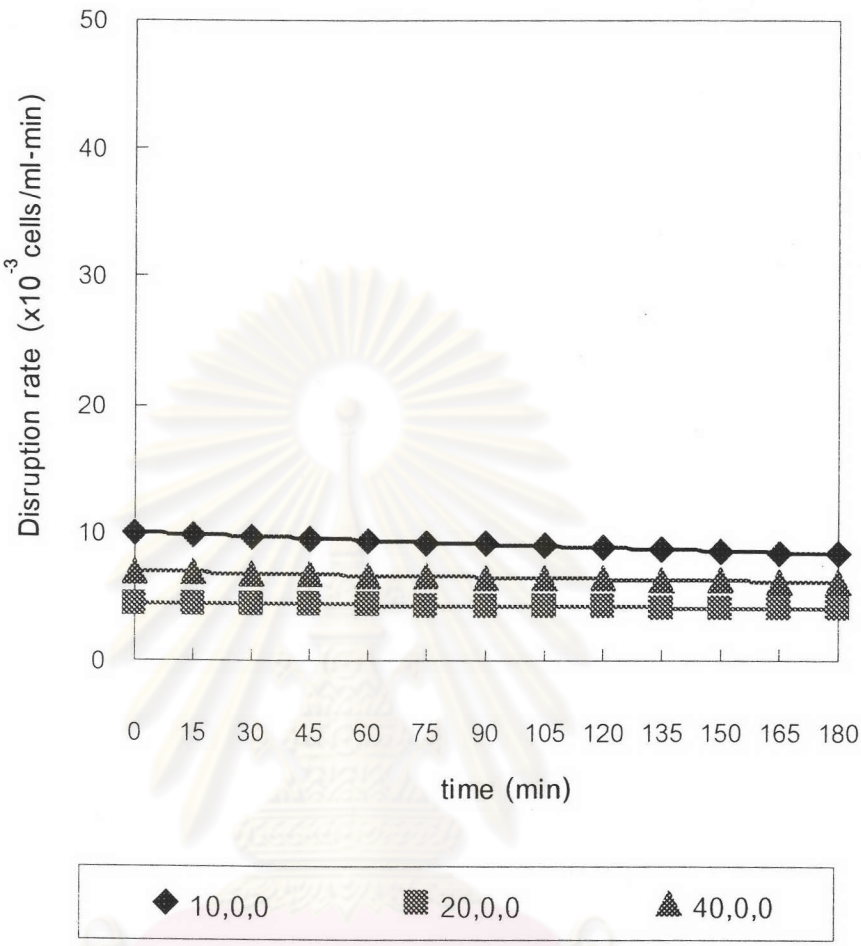

Figure 6-29. Rate of *Chroococcus* sp. cells disruption at various superficial gas velocities

U_g = 10, 20, 40 cm/min

U_l = 0 cm/min

N = 0 rpm

(U_g,U_l,N)

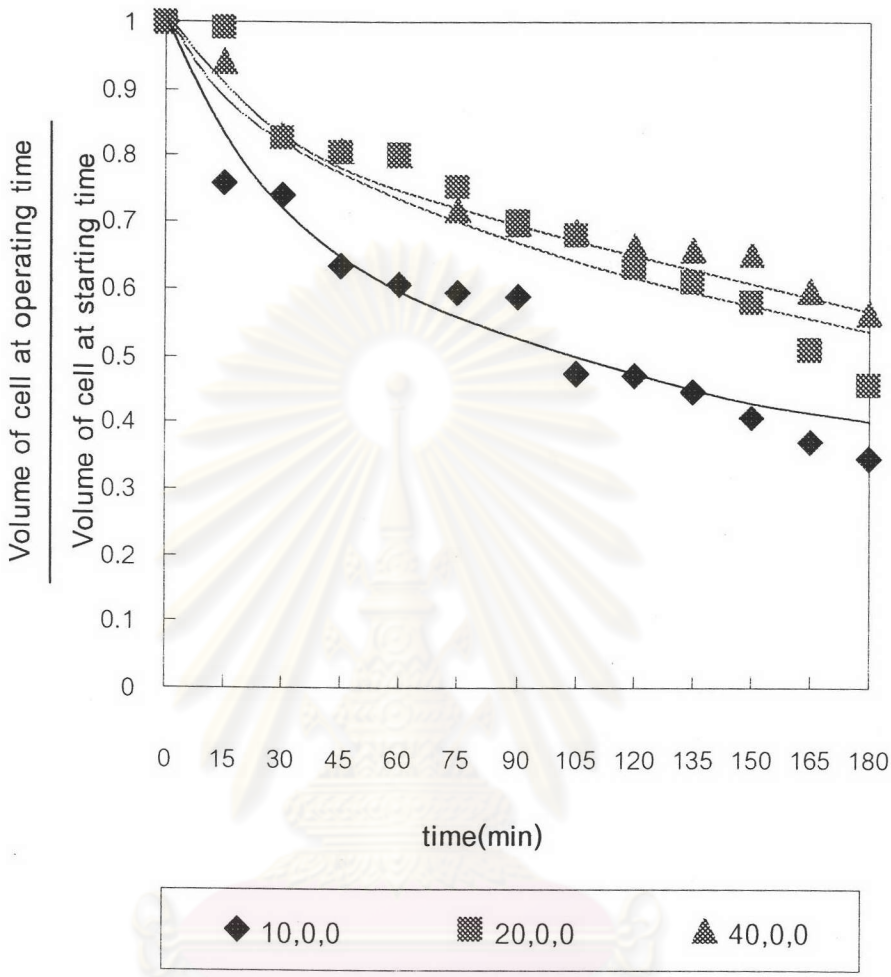

Figure 6-30. Ratio of volume of *Chroococcus sp.* cells measured between various operating time and starting time at various superficial gas velocities.

U_g = 10, 20, 40 cm/min

U_l = 0 cm/min

N = 0 rpm

(U_g,U_l,N)

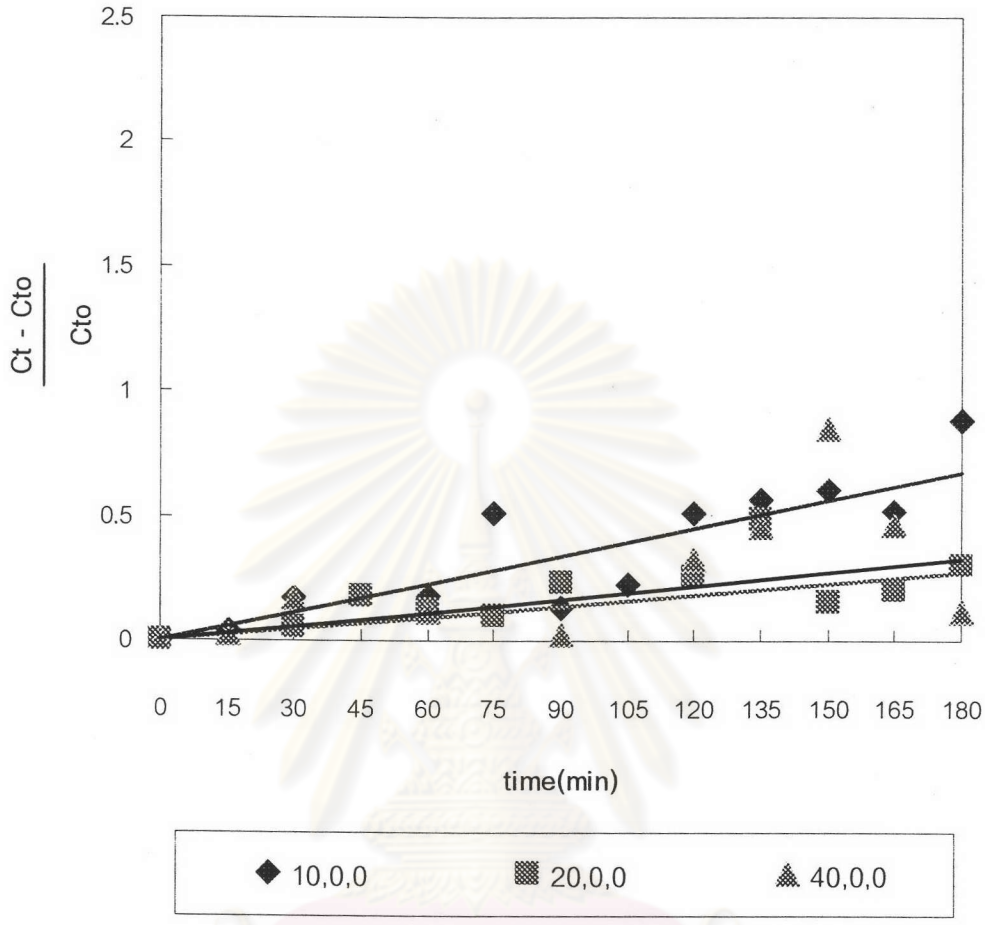

Figure 6-31. Ratio of Chlorophyll A of *chroococcus sp.* cells between operating time and starting time at various superficial gas velocities.

U_g = 10, 20, 40 cm/min

U_l = 0 cm/min

N = 0 rpm

(U_g,U_l,N)

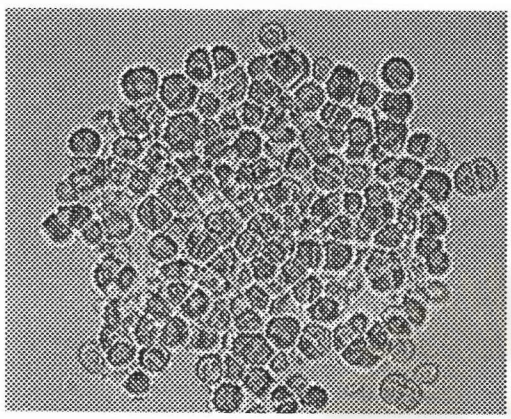

(a) U_g = 0 cm/min

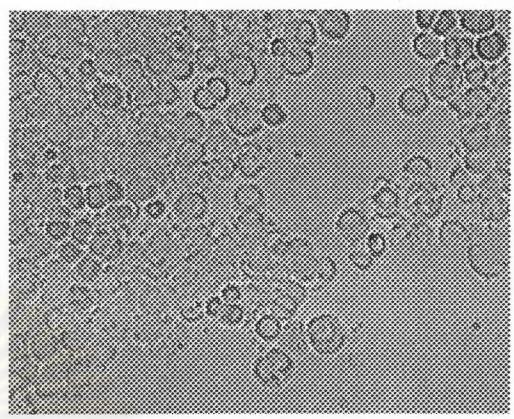

(b) U_g = 10 cm/min

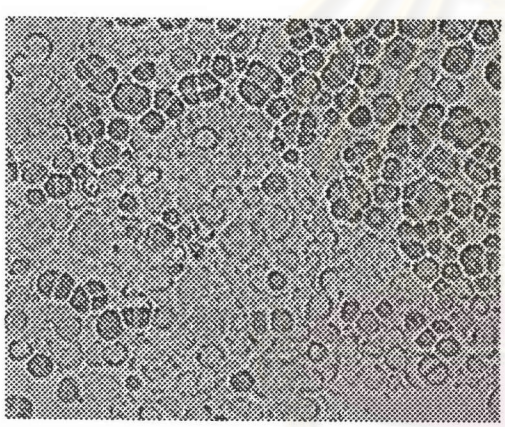

(c) U_g = 20 cm/min

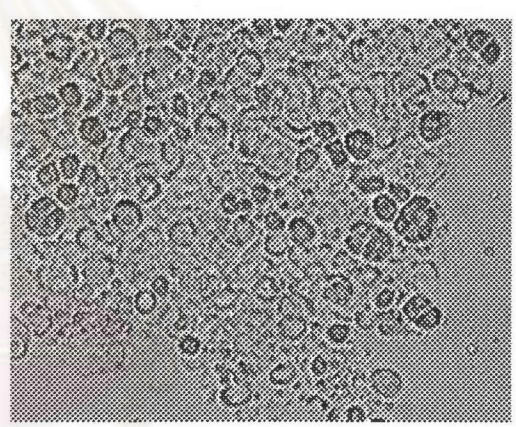

(d) U_g = 40 cm/min

Figure 6-32. Morphology of *Chroococcus sp.* (x400) at various superficial gas velocities.

U_g = 10, 20, 40 cm/min

U_l = 0 cm/min

N = 0 rpm

6.2.2 Combined effects of all variable on disruption of *Chroococcus* sp.

Under a condition of superficial gas velocity of 10 cm/min, with employing superficial liquid velocity of 10 cm/min and agitation speed of 3000 rpm, the percentage of cell disruption of 41.6% could be achieved (Figure 6-33). However, without introducing liquid flow and agitation, the percentage of cell disruption dropped to 22.3%. The result shows the same tendency as that of *Chlorella ellipsoidea*. Therefore it could be implied that the mechanism of *Chroococcus* sp. cell disruption might be the same as that the *Chlorella ellipsoidea* .

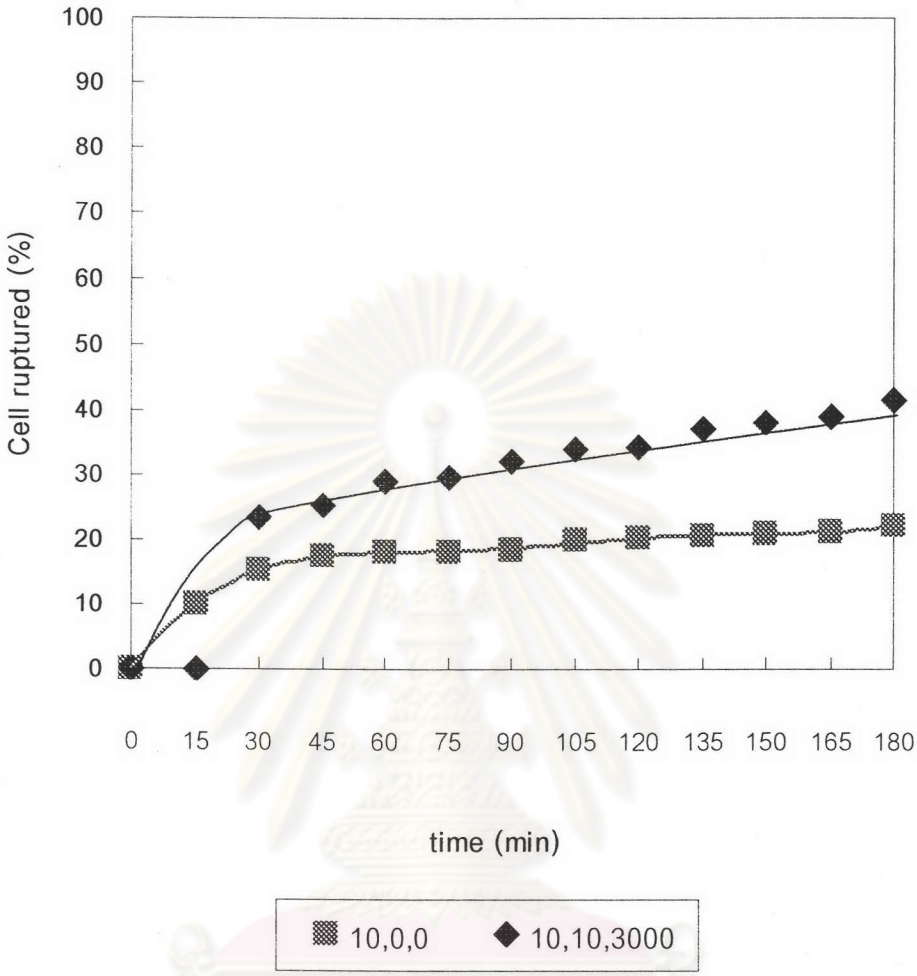

Figure 6-33. Percentage of *Chroococcus sp.* cells disruption compare between the condition had only superficial gas velocity and the condition had superficial gas and liquid velocity and agitation speed

U_g = 10 cm/min

U_l = 0, 10 cm/min

N = 0, 3000 rpm

(U_g,U_l,N)

6.3 Disruption of *Chlorococcum sp.* TISTR 8509

With the same reason, *Chlorococcum sp.* was also chosen because its cell structure was different from *Chlorella ellipsoidea* and *Chroococcus sp.*

6.3.1 Effect of Superficial Gas Velocity on Microalgal Cell Disruption

For *Chlorococcum* sp., the effect of superficial gas velocity at 10, 20 and 40 cm/min were investigated without employing superficial liquid velocity and agitation. Figure 6-34 shows that superficial gas velocity of 10 cm/min gave the optimal percentage of cell disruption at 15.6%. An increase in superficial gas velocity to 20 and 40 cm/min resulted in a decrease in cell disruption percentage, similar to those of *Chlorella ellipsoidea* and *Chroococcus* sp. However, the increasing superficial gas velocity had insignificant effect on the disruption rate of *Chlorococcum* sp. (Figure 6-35). In Figure 6-36, the increasing superficial gas velocity exhibited a slight influence on the ratio of cell volume at the end of operation to that of the starting. Similar trend could be observed for the ratio of Chlorophyll A released after starting operation (Figure 6-37). It could be implied that the excessively high superficial gas velocity, the cell disruption would be retarded due to the expansion of solid bed in the column. Morphological observation is also shown in Figure 6-38.

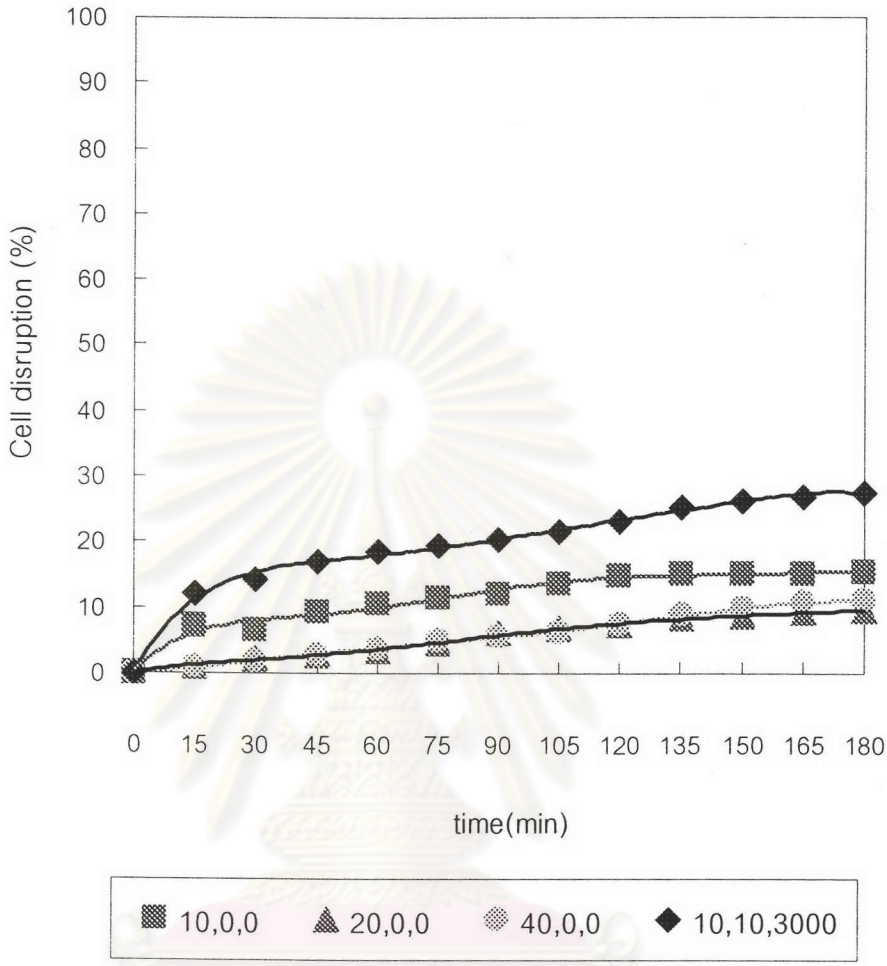

Figure 6-34. Percentage of *Chlorococcum sp.* cells disruption at various superficial gas velocities

U_g = 10, 20, 40 cm/min

U_l = 0 cm/min

N = 0 rpm

(U_g,U_l,N)

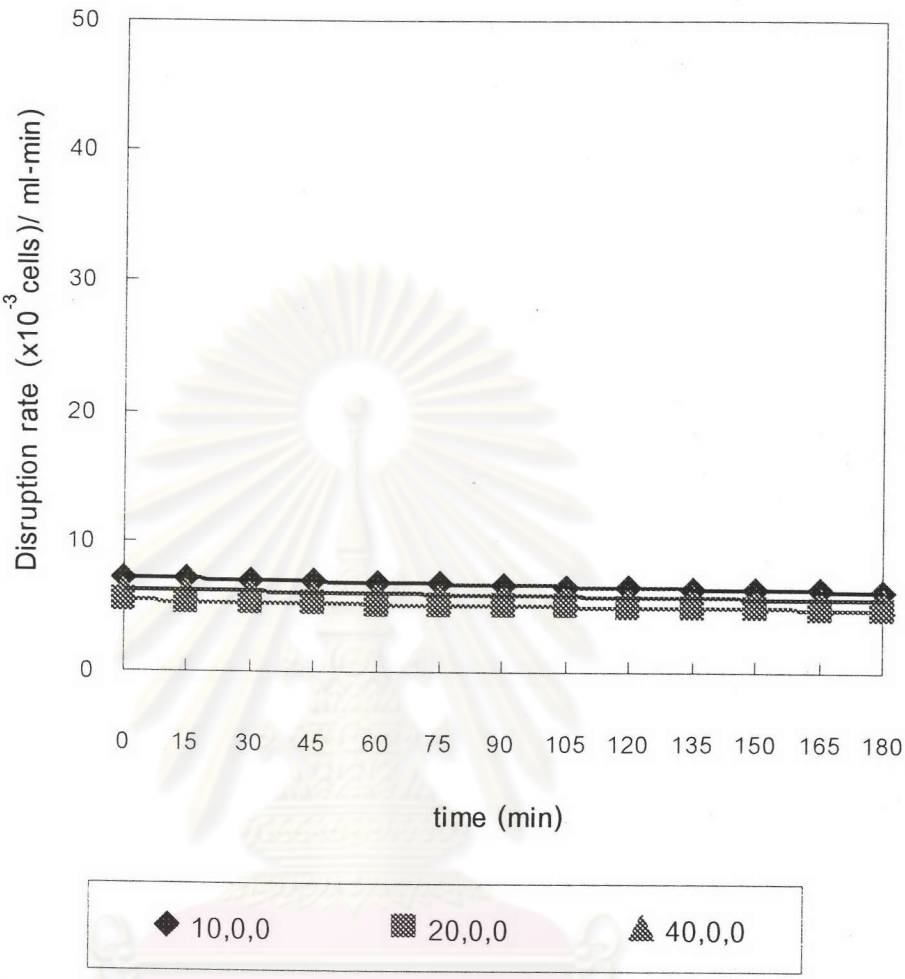

Figure 6-35. Rate of *Chlorococcum sp.* cells disruption at various superficial gas velocities

U_g = 10, 20, 40 cm/min

U_l = 0 cm/min

N = 0 rpm

(U_g,U_l,N)

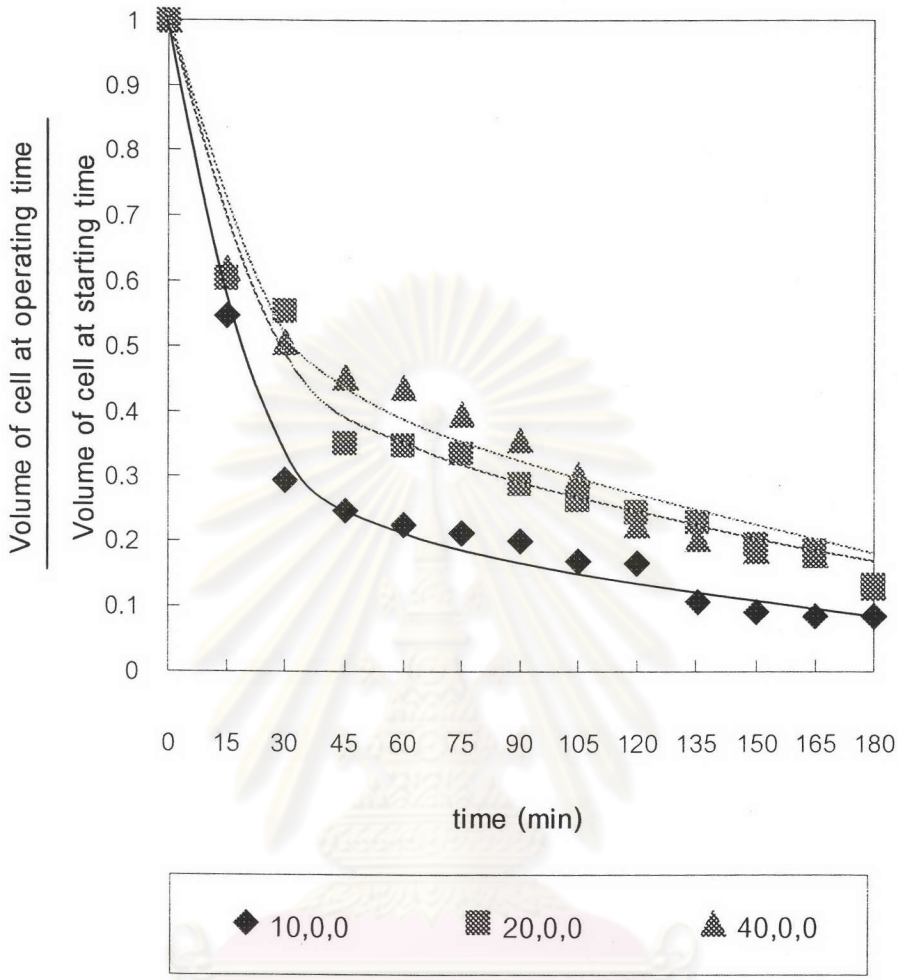

Figure 6-36. Ratio of volume of *Chlorococcum sp.* cells measured between various operating time and starting time at various superficial gas velocities.

U_g = 10, 20, 40 cm/min

U_l = 0 cm/min

N = 0 rpm

(U_g,U_l,N)

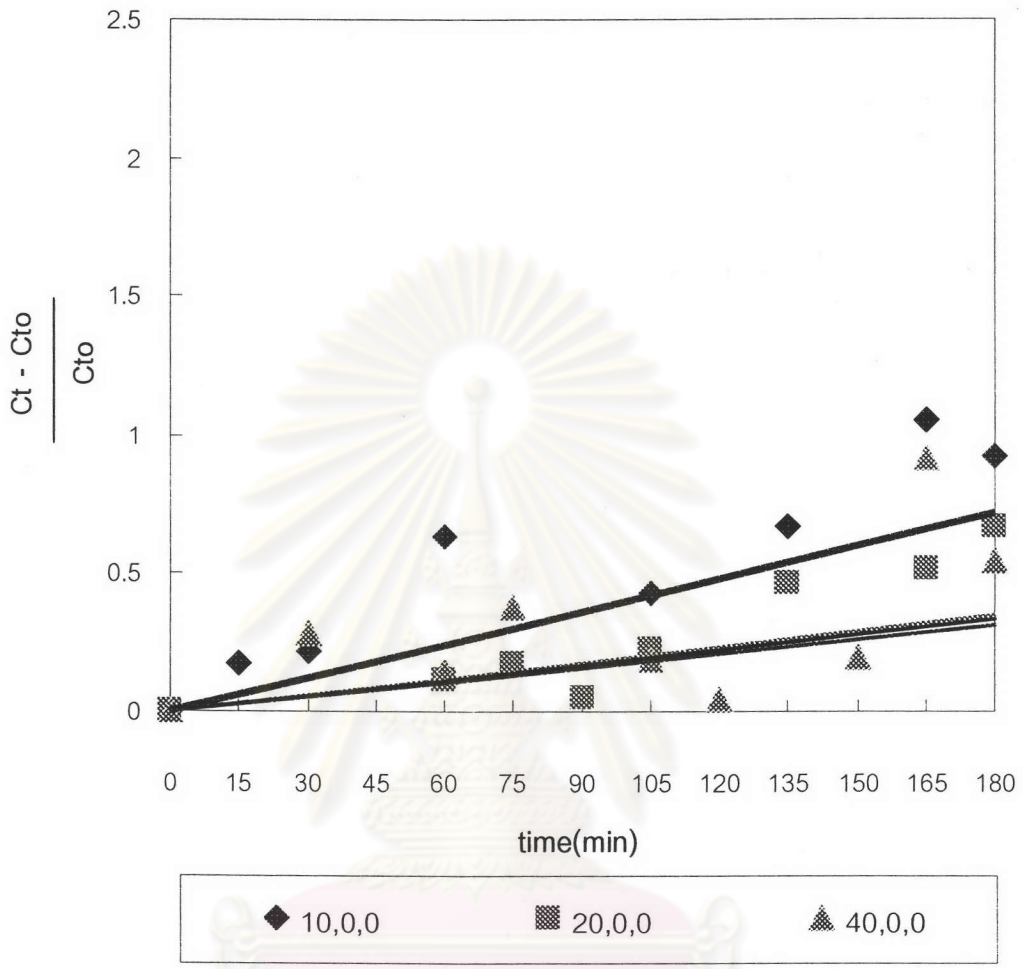

Figure 6-37. Ratio of chlorophyll a of *Chlorococcum sp.* cells between operating time and starting time at various superficial gas velocities.

U_g = 0, 10, 20, 40 cm/min

U_l = 10 cm/min

N = 3000 rpm

(U_g,U_l,N)

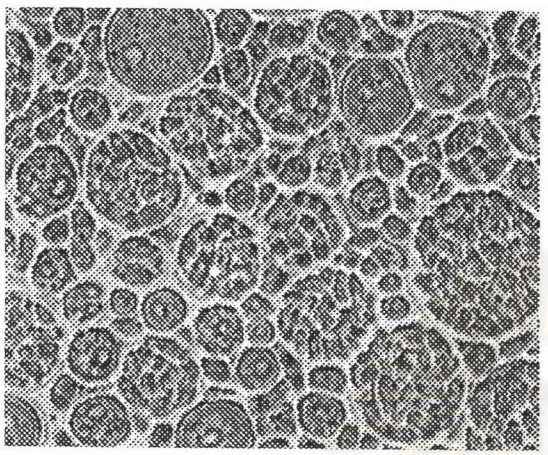

(a) U_g = 0 cm/min

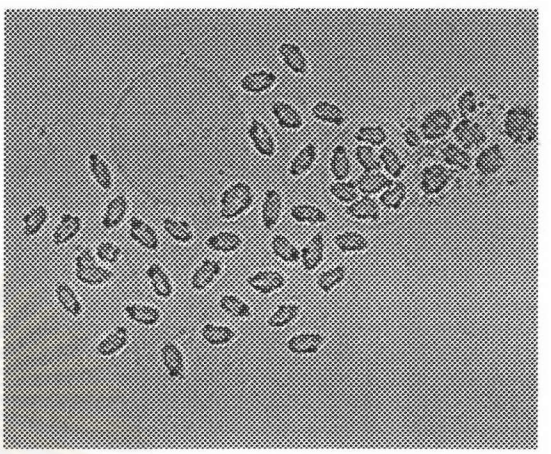

(b) U_g = 10 cm/min

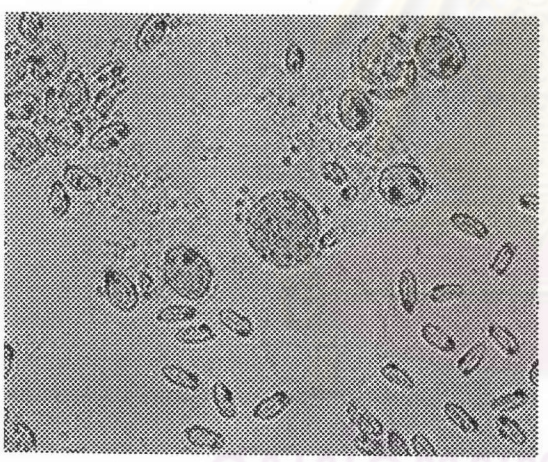

(c) U_g = 20 cm/min

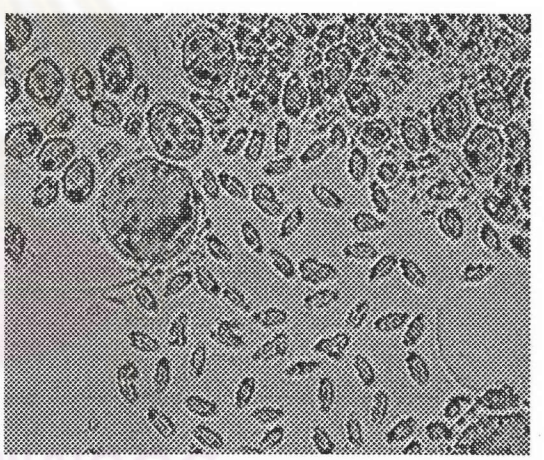

(d) U_g = 40 cm/min

Figure 6-38. Morphology of *Chlorococcum* sp. (x400) at various superficial gas velocities.

U_g = 10, 20, 40 cm/min

U_l = 0 cm/min

N = 0 rpm

6.3.2 Combined effects of all operating variable on disruption of *Chlorococcum* sp.

Figure 6-39 shows that when the liquid flow rate and agitation of 10 cm/min and 3000 rpm were introduced into the system with gas flow rate of 10 cm/min, the percentage of cell disruption were increased when compared with no introduction of liquid flow and agitation. However, the percentages of cell disruption in both cases are only 27.7 and 15.6, which was lower than that of *Chlorella ellipsoidea* and *Chroococcus sp.*

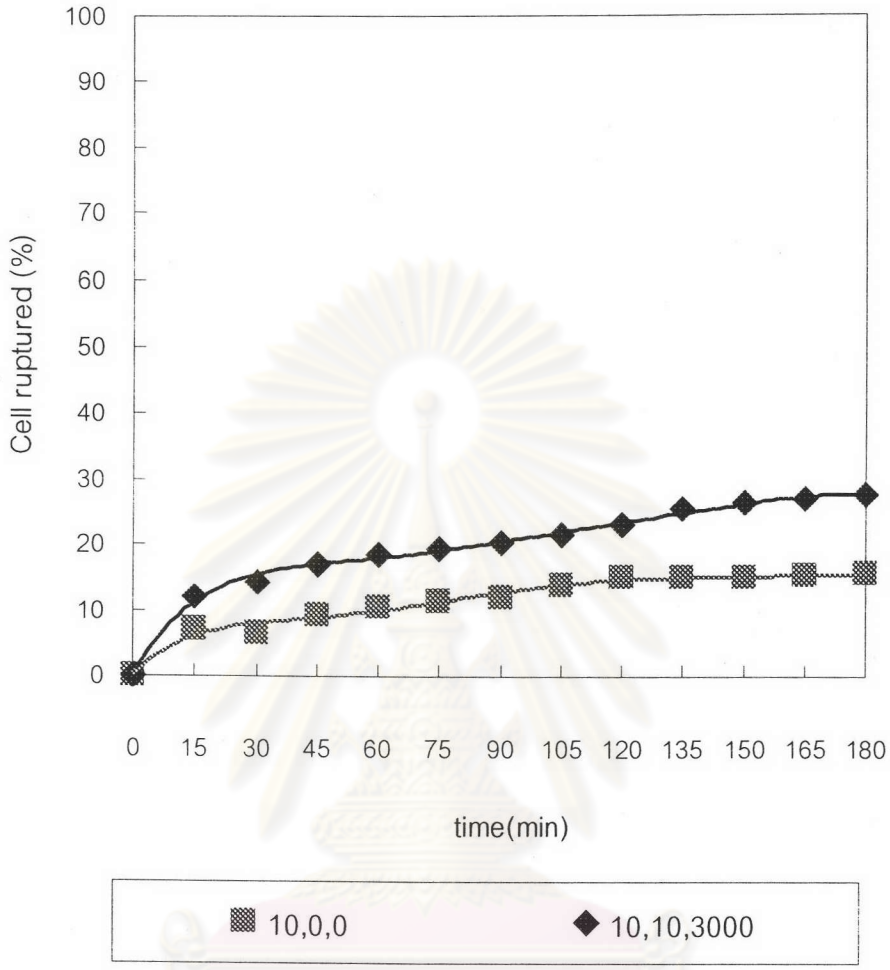

Figure 6-39. Percentage of *Chlorococcum sp.* (TISTR 8509) cell disruption compare between the conditions had only superficial gas velocity and the condition had superficial gas and liquid velocity and agitation speed cell disruption.

U_g = 10 cm/min

U_l = 0, 10 cm/min

N = 0, 3000 rpm

(U_g,U_l,N)

Disruption performance of *Chroococcus sp.* and *Chlorella ellipsoidea* in three-phase fluidized bed system under a condition of superficial gas, liquid velocity and agitation of 10 cm/min and 3000 rpm were considerated. Figure 6-40 shows the higher percentage of disruption of *Chlorella ellipsoidea* compared with *Chroococcus sp.* At 180 minutes, 93.6% of *Chlorella ellipsoidea* were disruptured while only 41.6% of *Chroococcus* sp. was broken. This result could be implied as dependence on the cell structure. *Chroococcus sp.* was sorted in cyanobacteria which have unicellular morphology. Its cell wall consists of two concentric layers, namely, a thin inner layer (cell wall) and a gelatinous thick outer layer (cell sheath). While *Chlorella ellipsoide.* was sorted in Chlorophyta having only single cell wall. Therefore, it could be expected that *Chlorella ellipsoidea* would be disrupted more easily.

For *Chlorococcum* sp., reproduction process would also be considered. *Chlorococcum sp.* colony consists of many small cells within reproductive cell wall. Therefore, the certain number of cell inside parental cell wall cannot be easily counted. The release of small cells from mother cell through rupture of mother wall, resulted in confusion in cell counting. Figure 6-41 shows size distribution at starting and ending of operation, it could be seen that all of large cells (ϕ = 8-28 μm) were disrupted and in turn only daughter cells ($\phi \cong$ 2-7 μm) existed at the end of operation.

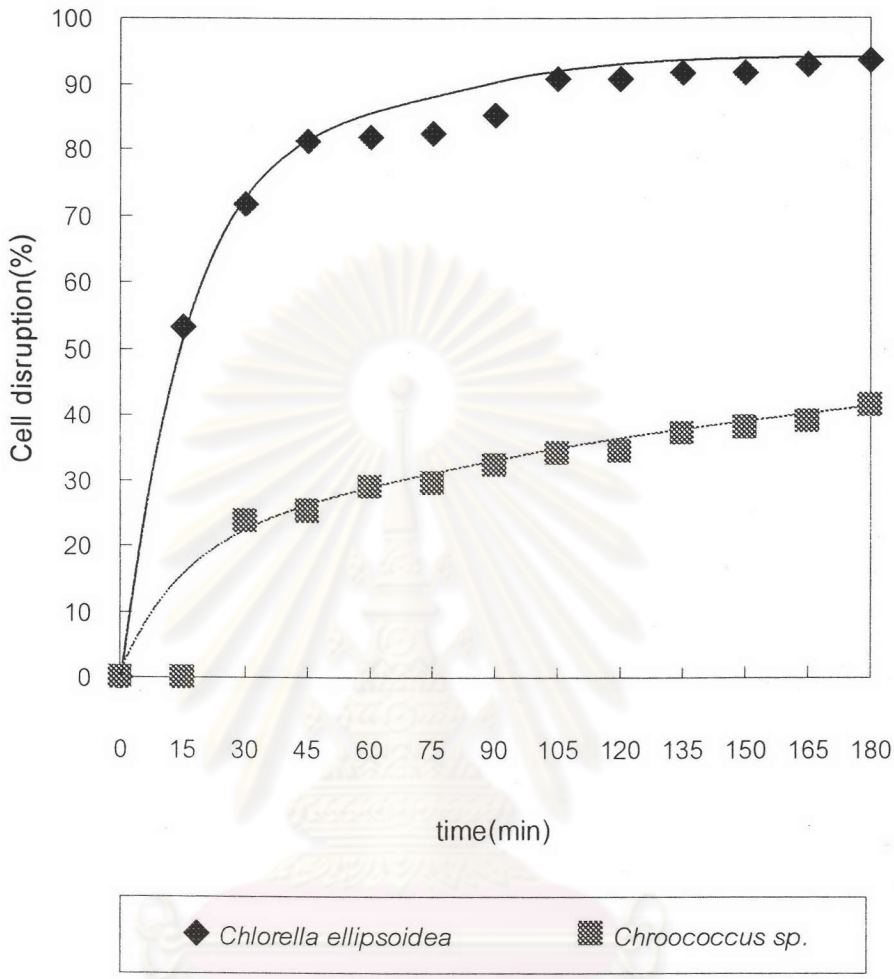

Figure 6-40. Percentage of cell disruption at various cell species. (*Chlorella ellipsoidea* and *Chroococcus* sp.)

U_g = 10 cm/min

U_l = 10 cm/min

N = 3000 rpm

(U_g,U_l,N)

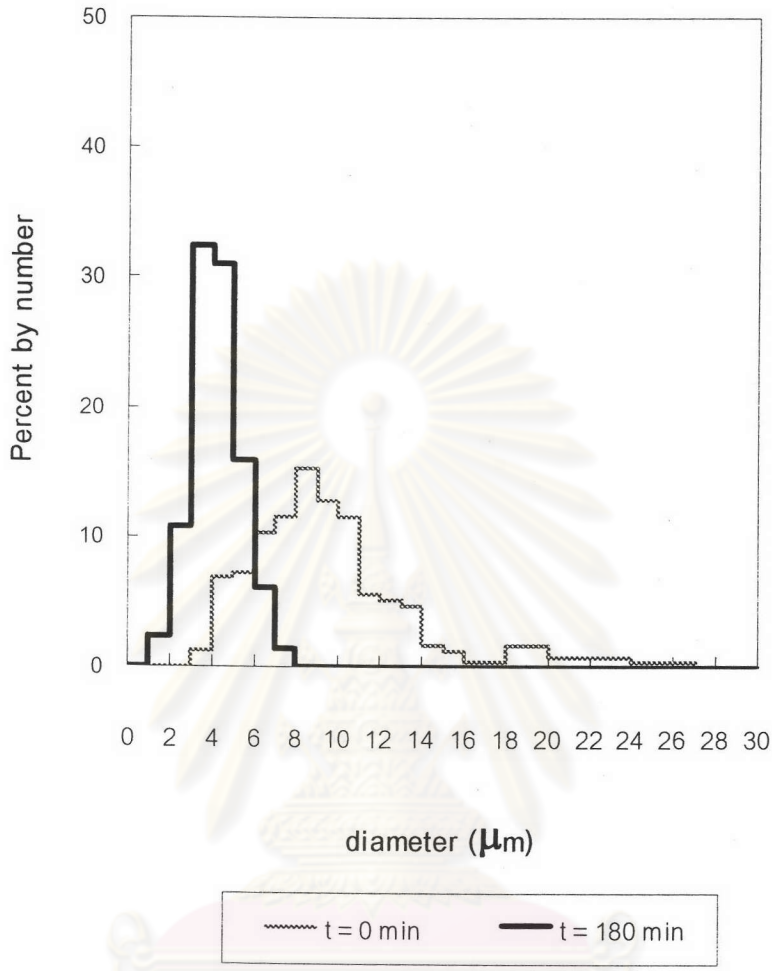

Figure 6-41. Size distribution of *Chlorococcum* sp. suspension at 0 and 180 minute

U_g = 10 cm/min

U_l = 10 cm/min

N = 3000 rpm

(U_g,U_l,N)

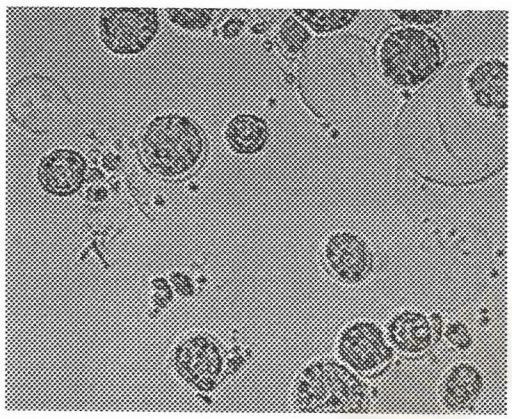

(a) t = 15 min.

(b) t = 90 min

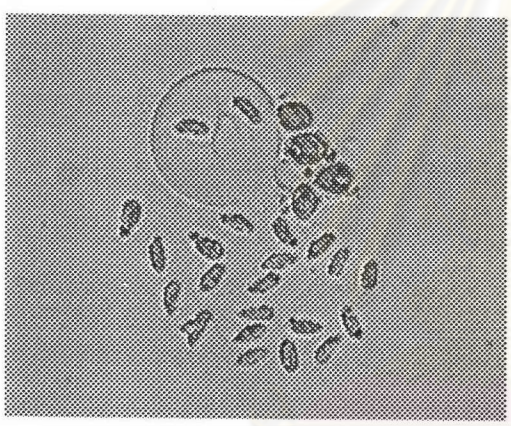

(c) t = 135

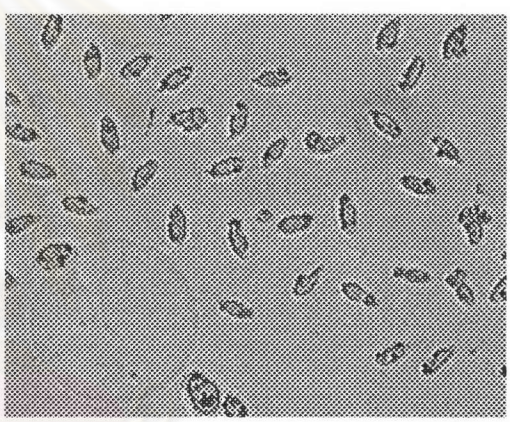

(d) t = 180 min

Figure 6-42. Morphology of *Chlorococcum sp.* (x400) at various operating time

U_g = 10cm/min

U_l = 10 cm/min

N = 3000 rpm